

SLOPE STABILIZATION AND PERFORMANCE MONITORING
OF I-35 AND SH-183 SLOPES USING
RECYCLED PLASTIC PINS

by

SANDIP TAMRAKAR

Presented to the Faculty of the Graduate School of
The University of Texas at Arlington in Partial Fulfillment
of the Requirements
for the Degree of

MASTER OF SCIENCE IN CIVIL ENGINEERING

THE UNIVERSITY OF TEXAS AT ARLINGTON

December 2015

Copyright © by Sandip Tamrakar 2015

All Rights Reserved



In Loving Memory of my Mom
Late Mrs. Ganga Tamrakar

Acknowledgements

I extend my heartfelt appreciations to my advisor, professor MD Sahadat Hossain for his guidance and constant motivation. He has been continuous guide through my research study. His meticulous planning of field work and extraordinary visualization of the field problems made this research study went through successfully. I am indebted to him and great forever for the help extended to me during my stay at University of Texas at Arlington.

I owe my sincere appreciation to Dr. Melanie Sattler and Dr. Xinbao Yu for accepting to be on my examination committee. I would like to thank them for the valuable advice and concepts during my research.

My special thanks to my colleagues in our research group. Particularly, I would like to thank Dr. Sadik Khan, for this valuable guidance and advice for the research. In addition, I would like to thank Ashraf, Masrur, Asif, Faysal, Dewan and Aaysuh for their help during instillation of the pin, field monitoring.

I am greatly indebted to my dad Gopi Tamrakar, and rest of my family Luna Sapkota, Sanjay Tamrakar, Najuma Maharjan for their cooperation, understanding and moral support.

November 18, 2015

Abstract

SLOPE STABILIZATION AND PERFORMANCE MONITORING
OF I-35 AND SH-183 SLOPES USING
RECYCLED PLASTIC PINS

Sandip Tamrakar

The University of Texas at Arlington, 2015

Supervising Professor: Sahadat Hossain

The United States earth retaining structure market exceeds 170 million square feet annually and there are over 50 different retaining systems to select from which are unique in design and construction. Depending on the type of retaining structure, unit costs vary from less than \$20 to in excess of \$250 per square foot. Selecting the technically appropriate and cost-effective system is often critical to project cost and schedule. The Recycled Plastic Pin (RPP) has potential to be utilized as a sustainable and cost effective option to stabilize the surficial slope failure. RPP have been successfully used in Missouri, Iowa and Texas to repair the surficial slope failure of highway embankment.

The current study summarized the remediation of shallow slope failure using RPP at two different slopes at DFW area. Two highway slopes, one located over SH-183 and SH-97 near DFW airport and second one over I-35 overpass at Mockingbird Lane in Dallas, Texas. Both of the slopes were modeled in PLAXIS and based on the numerical modeling, the number of RPP were determined. Sections of slope at each slope were reinforced with RPP and the performance of the slope was monitored using inclinometer and surveying instruments.

Based on the design methods, the calculated factors of safeties were in good agreement with the safety analysis results in numerical modeling.

Table of Contents

Acknowledgements	iv
Abstract	v
List of Illustrations.....	x
List of Tables.....	xiii
Chapter 1 Introduction.....	1
1.1 Background.....	1
1.2 Problem Statement.....	3
1.3 Research Objectives	3
1.4 Thesis Organizations	4
Chapter 2 Literature Review	5
2.1. Surficial Slope Failure.....	5
2.2. Repair Methods of Surficial Slope Failure	6
2.2.1 Rebuilding Slope	6
2.2.2 Geogrid Repair	7
2.2.3 Soil Cement Repair	8
2.2.4 Earth Anchors.....	8
2.2.5 Slope stabilization using geofom.....	9
2.2.6 Repair Using Launched Soil Nails.....	9
2.2.7 Micropiles	10
2.2.8 Plate Piles.....	10
2.3. Literature Review of Retaining Structures	11
2.3.1 Gabion Walls	11
2.3.2 Reinforced concrete retaining wall	12
2.3.3 Mechanically Stabilized Earth (MSE) Wall	13

2.3.4	Drilled Shaft Wall	14
2.3.5	Soil Nail Wall	15
2.4.	Recycle Plastic Pins	16
2.4.1	Engineering Properties of RPP	17
2.4.2	Long Term Engineering Properties of RPP	19
2.4.3	Creep of RPP	20
2.5.	Case Study Slope Stabilization at US 287 Slope	25
2.5.1	Site Investigation US 287	26
2.5.2	Analyses of Site Investigation Results	29
2.5.3	Slope Stability Analyses at US 287 Slope.....	30
2.5.4	RPP instillation at US 287 Slope	36
2.5.5	Performance Monitoring at US 287 Slope.....	38
2.5.5.1	Inclinometer.....	38
2.5.5.2	Topographic Survey.....	41
Chapter 3	Site Investigation	43
3.1	Site Investigation Background	43
3.2	Site Investigation of I-35 and Mockingbird Slope	43
3.2.1	Site Investigation I-35.....	45
3.2.2	Geotechnical Borings and Laboratory Testing	46
3.2.3	Resistivity Imaging	49
3.2.4	Slope Stability Analysis and Design of Slope Reinforcement	50
3.3	Site Investigation of SH 183 Slope	51
3.3.1	Project Background	51
3.3.2	Site Investigation SH 183.....	53
3.3.3	Geotechnical Boring and Laboratory Testing.....	54

3.3.4	Resistivity Imaging	56
3.3.5	Shear Strength Test	59
3.3.6	Slope Stability Analysis	60
Chapter 4	RPP Instillation and Slope Monitoring.....	63
4.1	Slope Stabilization at I-35 Slope.....	63
4.2	RPP instillation at I-35 Slope	64
4.3	Performance Monitoring of I-35 Slope.....	66
4.3.1	Inclinometer	67
4.3.2	Topographic Survey	69
4.3.3	Contour Survey	70
4.4	Slope Stabilization at SH 183 Slope.....	71
4.5	RPP instillation at SH-183 Slope.....	72
4.6	Performance Monitoring of SH 183 Slope.....	75
4.6.1	Topographic Survey	76
4.6.2	Contour Survey	76
4.7	Lesson Learned from instillation process	78
Chapter 5	Conclusion and Recommendation for Future Research	82
5.1	Summary and Conclusion	82
5.2	Recommendation for Future Research	82
References	84
Biographical Information	87

List of Illustrations

Figure 2-1 Slope Failure at US 287 North bound after heavy rainfall..... 5

Figure 2-2 Surficial Slope Failure Repair using Geogrids (Day, R. W., 1996)..... 7

Figure 2-3 Soil Cement repair of surficial slope failure (Day. R. W., 1996) 8

Figure 2-4 Slope stabilization using soil nail. (Titi and Helwany, 2007)..... 9

Figure 2-5 Slope Stabilization using plate pile (Short and Collins, 2006) 11

Figure 2-6 Gabion Wall used to prevent erosion control (HawyardBaker.com) 12

Figure 2-7 Cast in place wall placement (Quintanar, 2014)..... 13

Figure 2-8 Backfilling operation in wall 14

Figure 2-9 Construction of Drilled Shaft Retaining Wall. (www.fhwa.dot.gov)..... 15

Figure 2-10 Soil nail after instillation (www.worldpress.com) 16

Figure 2-11 Slope Stabilization using Recycle Plastic Pins (Khan, 2013)..... 17

Figure 2-12 Creep Curve for Recycle Plastic Pins (Malcolm, 1995)..... 21

Figure 2-13 RPP testing set up for a Creep (after Chen et al., 2007) 22

Figure 2-14 Typical deflection under constant axial stress (Chen et al., 2007) 23

Figure 2-15 Method to estimate flexural creep (after Chen et al., 2007) 24

Figure 2-16 Location of US 287 Slope..... 25

Figure 2-17 Observed cracks at US 287 slope along the crest (Khan, 2013) 25

Figure 2-18 Borings and Resistivity Imaging location (Khan, 2013) 26

Figure 2-19 Laboratory test results of US 287 27

Figure 2-20 Resistivity Imaging (a) RI-1 and (b) RI-2 at US 287 28

Figure 2-21 Resistivity Imaging Profile (a) Profile RI-1. (b) Profile RI-2 29

Figure 2-22 Slope Stability Analysis Using Plaxis,) (Khan, 2013) 32

Figure 2-23 RPP Layout at US 287 Slope (Khan, 2013) 33

Figure 2-24 Details of Slope Stabilization on US 287 Slope, (Khan, 2013)..... 34

Figure 2-25 Slope Stability Analyses using RPP (Khan, 2013)	35
Figure 2-26 RPP instillation photo at US 287	36
Figure 2-27 Layout of Inclinator at US 287 Slope	39
Figure 2-28 Displacement in Inclinator I-1 at US 287	39
Figure 2-29 Displacement in Inclinator I-3 at US 287	40
Figure 2-30 Layout of Survey Lines at US 287 Slope.....	41
Figure 2-31 Settlement at the crest of the US 287 Slope	42
Figure 3-1 Project Location of I-35 Slope	44
Figure 3-2 Observed Cracks at the crest of I-35.....	45
Figure 3-3 Borings and Resistivity Imaging Location at I-35.....	46
Figure 3-4 Laboratory test results of I-35.....	48
Figure 3-5 Resistivity Imaging Results of I-35 Slope	49
Figure 3-6 Slope Stability of I-35 Slope Using Plaxis	50
Figure 3-7 Project Location of SH 183.....	51
Figure 3-8 schematic of the failure condition	52
Figure 3-9 Slope Failure Photos at SH 183	53
Figure 3-10 Borings and Resistivity Imaging Location.....	53
Figure 3-11 Laboratory test results of SH-183.....	55
Figure 3-12 Location of Resistivity Imaging at SH 183.....	57
Figure 3-13 Resistivity Imaging Profiles of SH 183	58
Figure 3-14 Slope Stability Analysis of SH 183 Slope,	61
Figure 3-15 Slope Stability Analysis of SH 183,	62
Figure 4-1 proposed layout of the RPP for the Mockingbird slope	63
Figure 4-2 Slope stability analysis	64
Figure 4-3 RPP instillation at I-35	65

Figure 4-4 As-Built RPP layout of I-35 Slope.....	66
Figure 4-5 Displacement in inclinometer 1 at I-35	67
Figure 4-6 Displacement in inclinometer 2 at I-35	68
Figure 4-7 Displacement in inclinometer 3 at I-35	68
Figure 4-8 Settlement at the crest of the I-35 Slope	69
Figure 4-9 Contour Survey at I-35 Slope	70
Figure 4-10 Plan View of RPP layout at SH 183 slope.....	71
Figure 4-11 Section A-A of RPP layout at SH 183 Slope	72
Figure 4-12 RPP instillation at SH 183 Slope	73
Figure 4-13 As Built Layout of SH 183.....	74
Figure 4-14 As built Slope Stability analysis of Sections 1-1 and 2-2	75
Figure 4-15 Settlement at the crest of the SH-183 Slope	76
Figure 4-16 Contour Survey at SH-183 Slope	77
Figure 4-17 Conventional rig with hydraulic hammer	78
Figure 4-18 Iron nail being hammered into ground.....	79

List of Tables

Table 2-1 Uniaxial compression test results	18
Table 2-2 Four point bending test results	18
Table 2-3 Three point bending test results of RPP samples after weathering	20
Table 2-4 Three point bending test results of RPP after weathering	20
Table 2-5 Summary of typical compressive creep test	22
Table 2-6 Summary of Flexural Creep test result	24
Table 2-7 Soil Parameters used in Plaxis	31
Table 2-8 Average RPP Driving Time at US 287	37
Table 3-1 Soil Test Results of I-35.....	47
Table 3-2 Soil Parameters used for slope at I-35	50
Table 3-3 Soil Test Results of SH 183.....	54
Table 3-4 Shear Strength Test on Undisturbed Samples	59
Table 3-5 Shear Strength Test on Remolded Samples	60
Table 3-6 Soil Parameters used at SH 183	61
Table 4-1 Average RPP driving time.....	80

Chapter 1

Introduction

1.1 Background

Highway embankments underlain by expansive soils are susceptible to shallow surficial failure during the intense and prolonged rainfall events. Usually, failure occurs due to the increase in hydrostatic pressure resulting in reduction of the effective shear strength of the soil. Typically soils failure occurs due to an increase in pore water pressure and reduction of soil strength due to progressive wetting of soil near-surface soil. This condition is further intensified by moisture changes in the soil due to seasonal climatic fluctuations resulting in cyclic shrink and swell of the soil layer in the upper layer (McCormick et al., 2006).

During the summer, moisture in the top soil evaporates and shrinkage cracks are formed. These shrinkage cracks acts as a conduit for water infiltration from rainfall (McCormick and Short, 2006). Due to the wetting and drying cycle, surficial slope failures are predominant in the Dallas – Fort Worth area and possess a significant maintenance problem to the Texas Department of Transportation (TxDOT).

Costs associated with routine maintenance and repair of surficial slope failures are generally neglected and over looked although over time the total cost for maintenance of the slope end up costing much more than replacing the slope with retaining structure. The depths and plan dimensions of surficial failure vary with soil type and slope geometry and are generally characterized by sliding depths of less than 10 ft. However, 3 to 6 feet depth become very common (Loehr and Bowders, 2007). Tumer and Schuster, (1996) conservatively estimated the cost to repair of shallow slides which was equal or even greater than the costs associated with repair of major landslides. In addition, shallow failure often cause significant hazards to infrastructure such as guard

rail, shoulder, portion of roadways, and if not properly maintained, it requires more extensive and expensive repairs (Loehr et al., 2007).

The conventional slope stabilization technique includes installation of drilled shaft, replacement of slope using retaining wall, installation of soil nail and reinforcing the slope using geogrids. However, the conventional techniques are might be expensive in some instances for the repair of shallow slope failure. A recent innovation in stabilization of shallow slope failure includes the installation of recycled plastic pin (Parra et al., 2004), plate pile stabilization (McCormick and Short, 2006) and reinforcing slope using small diameter piles (Thompson and White, 2006) showed great potential in terms of cost and effectiveness.

In United States, earth retaining structure market exceeds 170 million square feet annually and there are over 50 different retaining systems to select from which are unique in design and construction (ASCE, 2013). Depending on the type of retaining structure, unit costs vary from less than \$20 to in excess of \$250 per square foot. Selecting the technically appropriate and cost-effective system is often critical to project cost and schedule.

The prevalent methods of slope stabilization techniques includes instillation of soil nail, reinforcing slopes with geogrids, installation of drilled shaft, and replacing the slope with retaining wall are among few. However, these methods might be expensive to repair of surficial slope failure to the department of transportation. A innovation in stabilization of shallow slope failure includes the instillation of Recycle Plastic Pin (Parra et al., 2004), Plate pile stabilization (McCormick and Short, 2006) and reinforcing slope using small diameter piles (Thompson and White, 2006) showed great potential in terms of cost and effectiveness.

Recycled Plastic Pin (RPP) had been utilized in the state of Missouri and Iowa as cost effective solution for the stabilization of shallow slope failure (Loehr and Bowders, 2007).

1.2 Problem Statement

Determining the appropriate retaining structure for a project is a complicated task which involves a thorough and educated process based on the experience of the engineer and the site condition. In addition, several considerations are required to be analyzed in order to achieve the desired result in terms of schedule of the project and budgeted.

Previous study was conducted to stabilize shallow slope failure using RPP and offered great potential as a sustainable and cost effective approach for the slope stabilization. In addition, there has been extensive research performed in retaining wall design, construction methods and construction cost of each type of retaining structures. Based on the previous studies performed, we know that using RPP on highway embankments is a sustainable and cost effective approach. This study was further implemented in two additional slopes with expansive soil and their field installation and performance of the slope is presented in this study. In addition, some cost comparison of the various types of retaining wall versus RPP has been performed. Therefore, the need of this study is essential for various types of department of transportation (DOT) to aid in their decision to either perform the regular maintains for the surficial slope failure, replace the slope with retaining structures which are comparatively expensive or install RPP, which is cost effective and environmentally friendly method .

1.3 Research Objectives

The overall objective of the current study was to establish a cost benefit of using recycle plastic pins over other retaining structure to stabilize the highway embankments

for a surficial slope failure. The specific objective of the study includes:

- Site Investigation and selection of study area
- Development of slope stabilization scheme using RPP based on FEM analysis.
- Instillation of RPP in the highway embankments
- Performance monitoring of the RPP at SH 183 and I-35 Slopes.

1.4 Thesis Organizations

Thesis is divided into six chapters that are summarized below:

Chapter 1 provides an introduction, present the problem statement and objective of the study.

Chapter 2 presents the literature review on different techniques of the slope stabilization for the surficial slope failure.

Chapter 3 describes the details of the site investigation of three highway slopes that are located over highway SH 183 and I-35. This chapter describes the site investigation detail that includes the soil borings, laboratory testing and geophysical investigations.

Chapter 4 presents the RPP instillation and performance evaluation of the reinforced slope. This chapter describes the methods utilized install the pins into the slope and the monitoring the performance of the stabilized slope.

Chapter 5 summarizes the conclusions from the current research and provides recommendation for future work.

Chapter 2

Literature Review

2.1. Surficial Slope Failure

Surficial slope failures are common in the areas with the expansive soils. Surficial slope failure refers to slope instabilities, which by definition, is a failure surface usually at depth of 4 feet or less (Day, R. W., 1989). These failures commonly occur in expansive soil after prolonged rainfalls followed by dry summer. During 2015, heavy rainfall followed by dry summer caused approximately four slope failure in Dallas – Fort Worth area. In many cases, the failure surface is parallel to the slope face as shown in Figure 2-1



Figure 2-1 Slope Failure at US 287 north bound after heavy rainfall.

Failure slip surface were reported varies based on the various literatures based on case study, but all studies show a shallow nature of slope failure. Titi and Halwany (2007), defines the failure surface depth of shallow slope to be equal to or less than 4 feet. According to Loehr et al. (2000), the depth of shallow slope failure is described as less than 10 feet. However, it generally varies between 3 to 6 feet (Khan, 2013).

According to Titi and Helwany (2007), the recommended shallow failure depth ranges from approximately 2 to 4 feet.

In general, surficial slope failure occurs when the rainfall intensity is larger than the soil infiltration rate and the rainfall last long enough to saturate the slope up to certain depth, which leads to the buildup of pore water pressure up to that depth (Abramson et al., 2002). The depth and extend of surficial slope failure depends on slope geometry, soil type, degree of saturation, seepage and climatic condition (Titi and Helwany. 2007).

Surficial slope failure can have huge impact on traffic flow due to the debris flows in to highway. Furthermore, surficial slope failures can have an enormous economic impact on the highway agencies such as district level department of transportations. Repair of slope failures are performed at the district and local levels as routine maintenance work. In many instances, these temporary repairs of slope failures generally occur after a year or two immediately after another heavy rainfall.

2.2. Repair Methods of Surficial Slope Failure

Various slope repair methods are available to stabilize the surficial slope failures. Selection of appropriate repair methods depends on the site access, slope steepness, availability of construction equipment, experienced contractors in the area and available budget. However, the most common method of repair of surficial slope failure is to push the failed soil mass back and compact.

Many other earthwork techniques involve reshaping the surface of the slope by benching the slope, flattening the steep slope. Techniques available in the literatures as well as few case studies to stabilize the surficial slope failures are tabulated below.

2.2.1 *Rebuilding Slope*

Rebuilding the slope is considered one of the economical methods and quick fix in the initial phase. It is performed as a routine maintenance work on failed slopes

throughout the country. However, this method is not economical in the long run as the maintenance cost of the slope will be very high for the duration of the design life of the slope is considered. This method is not very effective as shear strength of the re-compacted soil does not increase significantly (Titi and Helwany, 2007). In addition, social cost of the project will also be high as the impact of the slope failure every two to three year will increase the cost of the time delay in traffic and fuel cost to the tax payer will also increase.

2.2.2 Geogrid Repair

Geogrids are fabricated from high density polyethylene resins. According to Day, R. W., (1996), repair of surficial slope failures using geogrids materials consists of complete removal of the dialed soil. Benching the undisturbed soil below the slip surface, vertical and horizontal drains are installed to discharge water from the slope. Finally, the slope is built by constructing layers of geogrids and compacted granular materials. The schematic of Geogrid repair is presented in Figure 2-2.

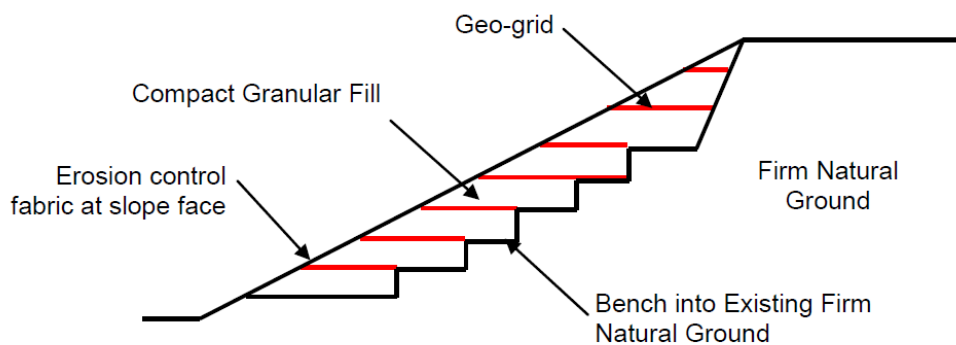


Figure 2-2 Surficial slope failure repair using Geogrids (Day, R. W., 1996)

2.2.3 Soil Cement Repair

Similar to geogrid repair, failure soil is excavated and removed. Soil below the failure plane is excavated and benched, drains are installed to remove the pore water. Granular Soil is mixed with cement up to 6 percent and compacted to at least 90 percent of the dry density (Day, R. W., 1997). The cement soil mix generally yield high shear strength resulting in higher factor of safety. The schematic of soil cement repair is presented in Figure 2-3.

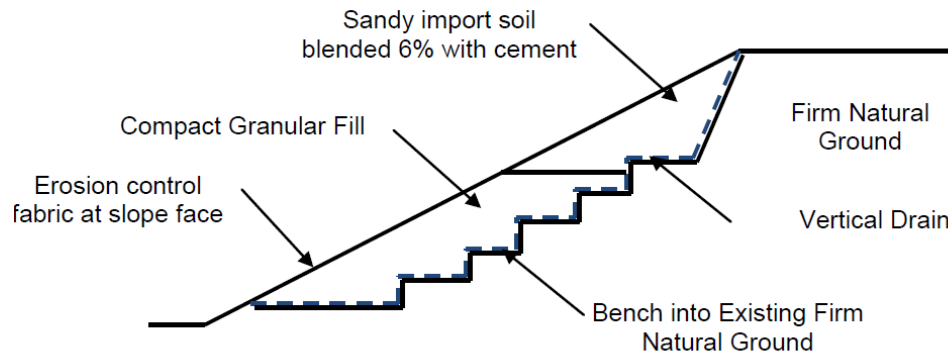


Figure 2-3 Soil cement repair of surficial slope failure (Day, R. W., 1996)

2.2.4 Earth Anchors

The earth anchoring system consists of mechanical earth anchor, wire rope and end plate. Earth anchors are recommended for slope stabilization and repair of surficial failure. This technique involves grading of failed slope, providing a turfing mat and then installing earth anchors. For installing the earth anchors, the anchors are first pushed into the soil below the failure surface. Wire tendon of the anchor is then pulled to move the anchors to its full working position resulting in the tendons to be locked against the end plate and the system is then tightened.

2.2.5 Slope stabilization using geof foam

Geofoam is highly used in geotechnical applications. It is used in many difficult sub soils condition around the world. Geofoams are formed with low-density cellular plastic solids that have been expanded as lightweight, chemically stable, environmentally safe blocks. The unit weight of geofoam ranged from 0.7 to 1.8 pcf and has compressive strength between 13 to 18 psi.

2.2.6 Repair Using Launched Soil Nails

Solid or hollow, steel bars are launched into the slope at a high speed using high pressure compressed air. Soil nail are installed at a staggered patterns throughout the failure zone, which provides the additional resistance along the failure plane as shown in Figure 2-4. Generally, hollow steel bars are 20 feet long with an outer diameter of 1.5 inch. Recommended minimum yielding strength of the bar is 36 ksi (Titi and Helwany, 2007). Slope surfaces are usually treated with erosion control mats or shotcrete after launching the soil nail.

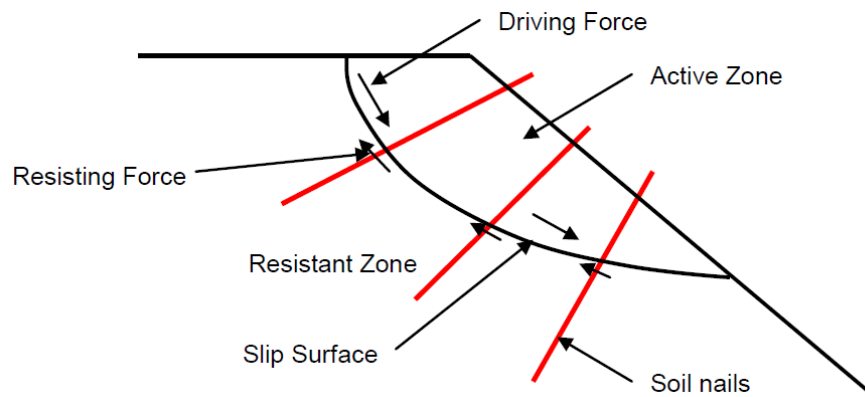


Figure 2-4 Schematic of repair of slope stabilization using launched soil nail.

(Titi and Helwany, 2007)

2.2.7 Micropiles

Micropiles (commonly known as pin piles or mini piles) are commonly used for foundations than slope stabilization (Taquinio and Pearlman, 1999). Micropiles have great potential to be used in slope stabilization. However, they have been used in very limited slope stability applications (Fay et al., 2012). Micropiles casing generally has a diameter between 3 to 10 inches. Using the drilling technique, the casing is advanced to the design depth. Reinforcement steels are inserted to the casing and grout is pumped into the casing.

2.2.8 Plate Piles

A study was conducted using Plate piles to stabilize surficial slope failure in state of California by Short and Collings (2006). Plate piles are installed vertically into the slope, which increases the resistance to sliding through reducing the shear stress. Generally, plate piles are 6 to 6.5 feet long and 2.5 by 2.5 inch steel angle iron section with 2 by 1 feet wide, rectangular steel plate welded to one end (McCormick and Short, 2006). Plate piles are driven into the potential unstable slope which has 2 to 3 feet soil over the stiffer soil or bedrock as shown in Figure 2-5. As the result of the plate, the driving force of the upper soil mass is reduced by transferring the load to stiffer subsurface soil or bed rock.

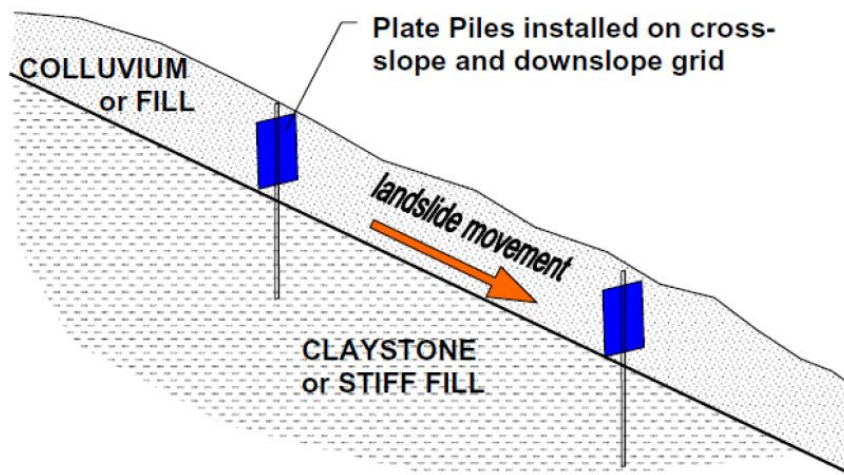


Figure 2-5 Slope stabilization using plate pile (Short and Collins, 2006)

2.3. Literature Review of Retaining Structures

Retaining structures are generally used to retain soils at a steep angle and are very useful when right-of-way is limited. Current heavy civil construction projects include a combination of the different types of retaining walls, each one of them determined based on its specific location or use. Retaining structures are selected based on the site specific soil conditions, height of the finished retaining structure, temporary or permanent use, space available for their construction and loads to withstand.

2.3.1 Gabion Walls

Gabion wall are made of heavy wire mesh and assembled on site, set in place, then filled with rocks. Horizontal and vertical wire support ties are used to keep the rocks inside the gabion basket. Gabions walls are composed of staked of gabions baskets and are considered unbound structures. Gabions walls can be used at the toe or the crest of the fill slope. Gabions wall can accommodate settlement without rupture and provide free drainage through the wall (Kandaris, P. M., 2007). Therefore, walls are used in the river embankments to prevent the soil from the embankments getting washed away and

prevent the landslides. According to Hayward Baker, Gabions wall are used to prevent the erosion control as shown in Figure 2-6.



Figure 2-6 Gabion wall used to prevent erosion control in Desoto, Texas

(Source HaywardBaker.com)

2.3.2 Reinforced concrete retaining wall

These walls are constructed from combination of concrete and reinforcement steel. The structural principle for these walls is the transformation of the lateral pressure into vertical load to the concrete footing, resisting the overturning by the weight of backfill mass over the footing heel. Cantilevered walls are the most optimized geometry among the cast in place concrete walls (Das, 2011). Cantilever wall use reinforced concrete and have a stem connected to a base of the slab.

Reinforced concrete retaining wall does not require highly specialized materials, equipment or craftsmanship. On the other hand, the horizontal space required to construct these walls is considerable and there are limitations of height both due to economic and structural considerations. Generally, if height of the retaining walls greater

than 25 feet, other retaining structure are recommended due to the increase in size of the concrete retaining wall. Design and specifications literature is extensive and readily available; therefore these constraints do not constitute a limitation on the specialization for the design and construction of these walls. Figure 2-7 presents the cast in place wall placement and subgrade preparation of reinforced concrete retaining wall.



Figure 2-7 Cast in place wall placement and subgrade preparation (Quintanar, 2014)

2.3.3 Mechanically Stabilized Earth (MSE) Wall

An MSE wall is a composite structure that is composed of backfill material, reinforcement, foundation and facing. The overall behavior of the entire wall is dependent on the interaction between all these components, especially between the reinforcement material and the backfill soil. These walls can be constructed easily, quickly, by non-expert workmanship and can be located in flood areas and retain substantial heights and loads when upward construction is needed. However, these are flexible walls that can present considerable movement which can sometime results in failures. Special care must be taken when developing the specifications, quality control, performance monitoring, backfill materials, drainage, corrosion of reinforcement and construction damage (Hossain et al. 2012). For example, Kibria et al (2014) analyzed an MSE wall in Lancaster, Texas that accumulated horizontal movements between 300 and 450 mm

during the years 2004–2009 due to primarily inadequate reinforcement lengths. As in the case of the cantilever walls, design and specifications literature is also wide and the need for specialized knowledge is not a constraint for this type of wall. Figure 2-8 shows the backfilling operation and metal strip placement over the lift of TxDOT materials.



Figure 2-8 Backfilling operation in wall, strip placement over after the lift and loader compacting the backfill soil.

2.3.4 *Drilled Shaft Wall*

A drill shaft wall is a structure composed by a sequence of closely spaced reinforced concrete cylinders drilled in the ground. Different configurations of spacing, size, length and reinforcement can be designed depending on the groundwater conditions, soil type, height and loads to support (Bierchwale et al. 1981). These walls appear as an appropriate solution where a strict movement control is necessary due to lateral forces in slope. These walls have a high cost, low production rate and require of specialized machinery and workmanship as well as design processes. Figure 2-9 Shows the drilled shaft retaining wall construction.



Figure 2-9 Construction of drilled shaft retaining wall. (Source fhwa.dot.gov)

2.3.5 Soil Nail Wall

Soil and Rock nail walls have been widely used during construction on highway embankments as an earth retaining structure for both temporary and permanent applications. This earth retention system is based on the use of steel bars inside drilled holes that are later filled with grout over the exposed face of the cut (Hayward Baker, 2013). These walls are constructed downward under normal circumstances. A drainage system is placed over the exposed soil cut in order to collect and evacuate the groundwater behind the wall. Steel plates and nuts retain the steel bars inside of the ground, therefore providing a passive resistance (Hayward Baker, 2013). The final step is the coverage of the exposed face and drainage strips by application of a layer of pneumatically placed concrete (shotcrete) and/or precast concrete panels. Figure 2-10 shows the construction of Soil Nail Wall.



Figure 2-10 Soil nail after instillation (Source Wordpress.com)

2.4. Recycle Plastic Pins

Recycled plastic pin, which is commercially known as, recycled plastic lumber are manufactured using post- consumer waste plastic, has been proposed as an acceptable material for use in the construction of docks, piers and bulkheads. Plastic lumber is also marketed as one of the environmentally preferable materials. Based on environmental and life cycle cost analysis standpoint, use of RPPs are under consideration as structural materials for marine and waterfront application (Khan, 2013). RPP require no maintenance, is resistant to moisture, corrosion, rot and insects. It is made of recycled, post-consumer materials and helps reduce the problem associated with disposal of plastics. Typically, 50% or more of the feedstock used for plastic lumber composed of polyolefin in terms of high density polyethylene (HDPE), low density polyethylene (LDPE) and polypropylene (PP). The polyolefin acts as an adhesive and combine high melt plastics and additives such as fiberglass, wood fibers within a rigid

structure. Figure 2-11 shows the schematics of slope stabilization using Recycle Plastic Pins.

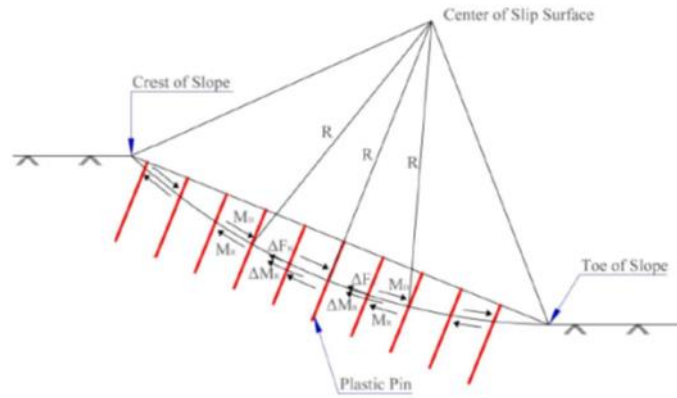


Figure 2-11 Slope stabilization using Recycle Plastic Pins (Khan, 2013)

Recycle plastic pins has been used in Missouri and Iowa as a cost effective solution for slope stabilization compared to conventional techniques (Loehr and Bowders, 2007). RPPs are lightweight materials and are installed in the failed area to provide resistance along the slipping plane to increase the factor of safety.

2.4.1 Engineering Properties of RPP

Different engineering properties of RPP were evaluated by Bowders et al., (2003) of wide varieties of production standards and to develop specifications for the slope stabilizations. Uni-axial compression tests and four point flexural tests were performed. Samples from three manufacturers we collected and tested. The experimental results for uni-axial compression and four point bending tests are presented in Tables 2-1 and 2-2, respectively.

Table 2-1 Uniaxial compression test results (Bowders et al., 2003)

Specimen Batch	No. of Specimen tested	Nom. Strain Rate (%/min)	Uniaxial Compressive Strength (ksi)		Young's Modulus, E1 % (ksi)		Young's Modulus E5 % (ksi)	
			Avg.	Std. Dev.	Avg.	Std. Dev.	Avg.	Std. Dev.
A1	10	-	2.76	0.13	133.7	7.7	56.6	3.9
A2	7	0.005	2.9	0.12	186.4	10	54.8	2.2
A3	6	0.006	2.9	0.13	176.9	15.7	52.6	3.9
A4	3	0.004	2.9	0.13	199.7	23.9	52.6	3.6
A5	4	0.006	1.74	0.15	93.5	23.1	32.6	2.5
A6	4	0.006	1.89	0.13	114	15.4	34.5	4.9
B7	2	0.007	2.03	0.07	78.5	5.2	38.9	0.4
B8	2	0.006	2.32	0.06	93.3	0.1	44.7	0.1
C9	3	0.0085	2.47	0.16	77.3	12.2	56.1	5.8

Table 2-2 Four point bending test results (Bowders et al., 2003)

Specimen Batch	No of Specimens Tested	Nom. Def. Rate (in/min)	Flexural Strength (ksi)	Secant Flexural Modulus E1% (ksi)	Secant Flexural Modulus E5% (ksi)
A1	13	-	1.6	113	96
A4	3	0.168	2.6	201.3	-
A5	3	0.226	1.6	103.1	73.1
A6	4	0.143	1.5	92	64.3
B7	1	0.159	1.3	78.9	61.6
B8	1	0.223	-	118.4	-
C9	2	0.126	1.7	100.2	80.2

2.4.2 Long Term Engineering Properties of RPP

Long term engineering properties of RPP was studied by Breslin et al. (1998). Plastic lumber samples used in the deck for over two year period was tested in the laboratory. At the initial process, the author investigated the initial engineering properties of recycled plastic lumber which was manufactured using a continuous extrusion process. Plastic lumbers were collected at regular interval for two years of monitoring period. Lumber did not face severe traffic load however, it was subjected to two summer cycles where the highest temperatures and UV intensities had taken place. Noticeable change such as warping, cracking and discoloration in the plastic was not observed.

The effect of the weathering on the mechanical behavior of recycled HDPE based plastic lumber was investigated by Lynch et al. (2001). During the study, flexural properties of weathered deck boards were obtained by performing flexural tests in three point loading, for comparison to original flexural properties according to ASTM D 796. The three point bending test results of the weathered sample are presented in Tables 2-3 and 2-4

Table 2-3 presents the flexural properties of RPP when the exposed side was tested in tension. Table 2-4 presents the flexural properties when the unexposed side was tested in tension. Modulus increased by 28 percent from the original when exposed site was tested in tension and increased by 25 percent when unexposed side was tested in tension.

Table 2-3 Three point bending test results of RPP samples after weathering (Exposed side was tested in tension) (Lynch et al., 2001)

Sample	Modulus (ksi)	Strength at 3% strain (ksi)	Ultimate strength (ksi)
1A	240.47	2.77	3.43
2A	213.79	2.48	3.12
3A	200.88	2.44	2.86
4A	214.22	2.55	3.32
5A	227.42	2.73	3.31
Average	219.30	2.59	3.21

Table 2-4 Three point bending test results of RPP after weathering (Unexposed side was tested in tension) (Lynch et al., 2001)

Sample	Modulus (ksi)	Strength at 3% strain (ksi)	Ultimate strength (ksi)
1B	217.56	2.77	3.49
2B	204.50	2.47	3.05
3B	190.29	2.45	3.05
4B	219.30	2.43	3.11
5B	234.67	2.76	3.25
Average	213.21	2.58	3.19

2.4.3 Creep of RPP

The recycled plastic lumber is nearly isotropic material with considerable strength, durability and workability. It can be reinforced and formed as composite materials. It is visco-elastic materials susceptible to creep and increased deflection with time under a static sustained load. Malcolm, M. G. (1995) conducted a study on the creep behavior of a 1 ½ X 3 ½ inch recycled plastic lumber sample that was subjected to a sustained min span bending stress of 516.7 psi that produced the creep curve as

presented in Figure 2-12. It is important for plastic lumber to maintain in low stress level for sustained load.

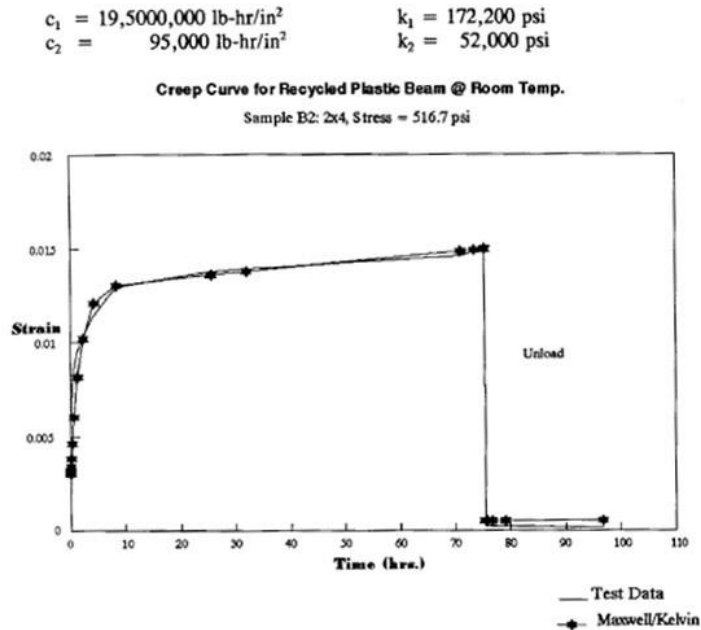


Figure 2-12 Creep curve for Recycle Plastic Pins (Malcolm, 1995)

Chen et al., (2007) had performed a study on the creep behavior of RPP. Due to variety of manufacturing process and constituent, the engineering properties of commercially available materials vary substantially. The polymeric materials are durable in terms of environmental degradation; however, they can exhibit higher creep rates compared to other structural materials such as timber, concrete or steel.

Chen et al., 2007 tested 3.5 inch by 3.5 inch rectangular specimen from 3 different manufacturers to evaluate the creep behavior. During the study, a total of 8 samples were tested. Tests were performed on specimens from three manufacturers. The compressive creep tests were performed on specimens cut from full size RPP, with nominal dimensions of 3.5 inch squares by 7 inch in length. The compressive load was applied using a spring with a 3 kip/ft spring constant. All specimens were tested at room temperature of 21 °c. On

the other hand, the flexural creep responses were performed on scaled RPP of 2 X 2 X 24 in. The test set up for both compressive and flexural creep is presented in Figure 2.13. The flexural creep test was performed at different temperature (21, 35, 56, 68, and 80°C). The study considered Arrhenius method to estimate the long term creep behavior.

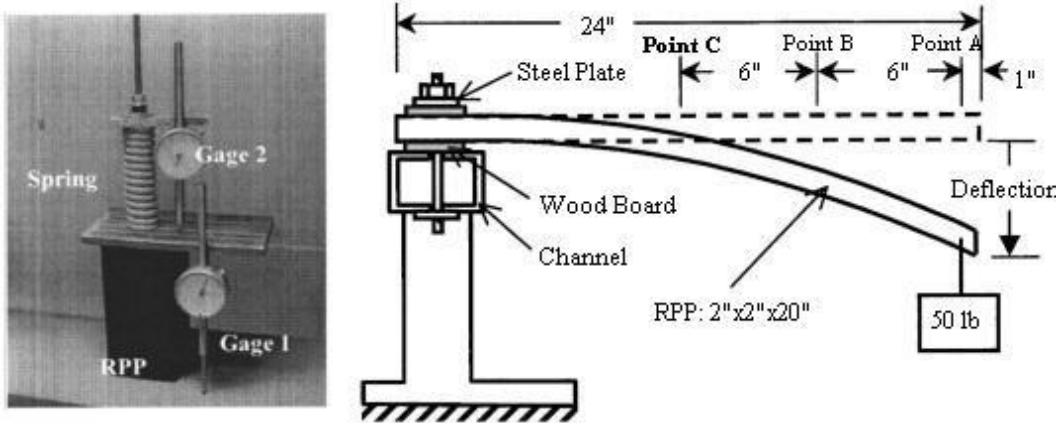


Figure 2-13 RPP testing set up for a Creep (after Chen et al., 2007)

A typical plot of deflection vs. time for the compression creep and the compression creep results are presented Table 2-5 and Figure 2-14, respectively. Figure 2-14 indicated that the primary creep was completed within one day after the load applied for all specimens. Secondary creep occurred after primary creep and continued for a year at a steady rate.

Table 2-5 Summary of typical compressive creep test (Chen et al., 2007)

Manufacturing	Number of Specimens	Creep Stress (psi)	Ratio of Creep stress to compressive strength	Maximum Creep Strain (%)
A3	2	105	3.7	0.1
A6	2	100	6.3	0.1
B7	1	110	5.3	0.4
C9	1	120	5.1	0.4

Deflections under constant axial stress

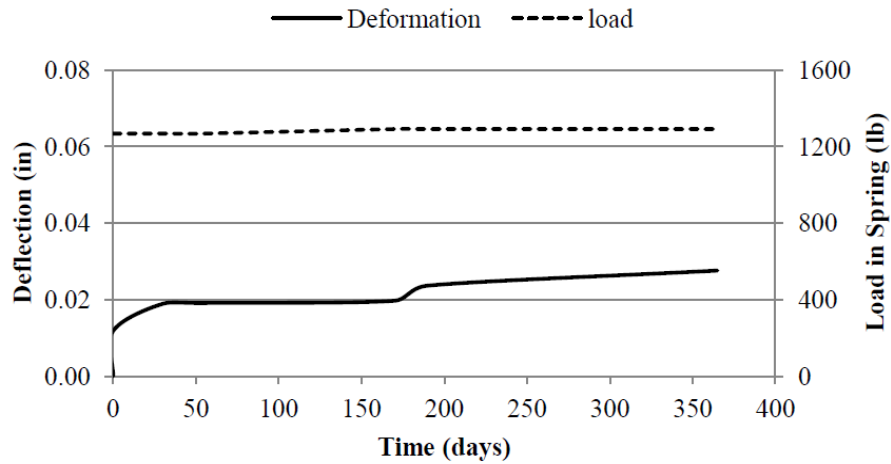


Figure 2-14 Typical deflection under constant axial stress (Chen et al., 2007)

The flexural creep test results are presented in Table 2-6. As the temperature increased, the time to reach failure decreased for the same load condition. Results showed that the loading levels, along with temperature, affected the creep behavior of the recycled plastic specimens. In addition, it was presented that the higher the load levels or the closer to the ultimate strength of the material, the faster the creep rate and shorter time to reach failure. Based on the study, the author presented a method to investigate the design life of RPP, based on percentage load mobilization as presented in Figure 2-15. The higher the mobilized loads, the design life of RPP become susceptible to creep failure. The author suggested to perform effective design procedure to reduce the load mobilization which could be obtained through increasing the number of RPP thereby, reducing the spacing, changing the constituents or changing the section of RPP to increase moment of inertia.

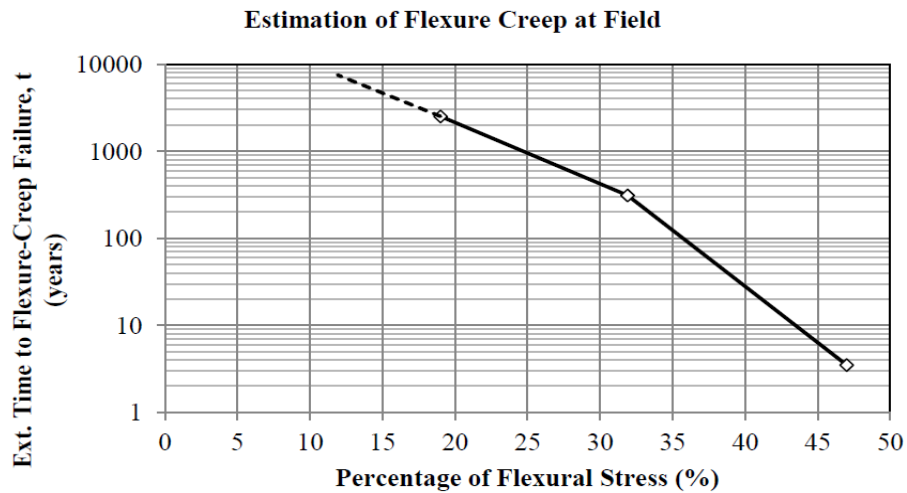


Figure 2-15 Method to estimate flexural creep in the field (after Chen et al., 2007)

Table 2-6 Summary of Flexural Creep test result (Chen et al., 2007)

Loading Conditions	Temperature (°C)	Number of Specimens tested	Average time to reach failure (days)	Comments
44 N at 5 points	21	2	1.185 ^a	Not failed
	56	2	195	failed
	68	2	3.5	failed
	80	2	0.8	failed
93 N single points	21	2	1.185 ^a	Not failed
	56	2	574	failed
	68	2	17.5	failed
156 N at single points	80	2	8.5	failed
	21	2	1.185 ^a	Not failed
	56	2	71.5	failed
	68	2	0.6	failed
222 N at single points	80	2	0.8	failed
	21	2	1.185 ^a	Not failed
	56	4	200	failed
	68	2	3.1	failed
	80	2	0.4	failed

^a Last day of testing: specimen not ruptured

2.5. Case Study Slope Stabilization at US 287 Slope

Khan, 2013 performed a study using RPP to stabilize US 287 slope. The slope is located over Highway US 287, near St. Paul overpass in Midlothian, Texas as presented in Figure 2-16. The maximum height of the slope is approximately 30 feet with 3(H):1(V) slope. Cracks were observed in 2010 on the shoulder of the highway slope as shown in Figure 2-17. The slope was constructed in 2003 – 2004 from the fill soil in the vicinity of the project site.

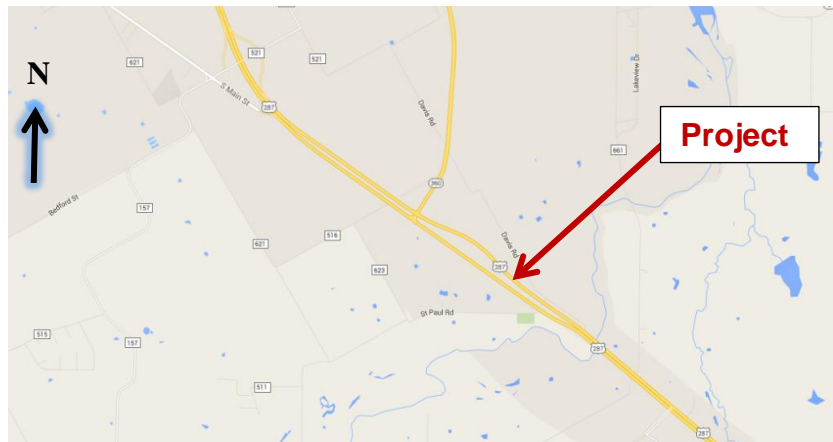


Figure 2-16 Location of US 287 slope.



Figure 2-17 Observed cracks at US 287 slope along the crest (Khan, 2013)

2.5.1 Site Investigation US 287

Geotechnical and geophysical investigation was conducted at US 287 on October 2010. Three geotechnical Borings and two 2D Resistivity Imaging (RI) were conducted in the site. The layout of the Borings and the location of RI profiles are presented in Figure 2-18.

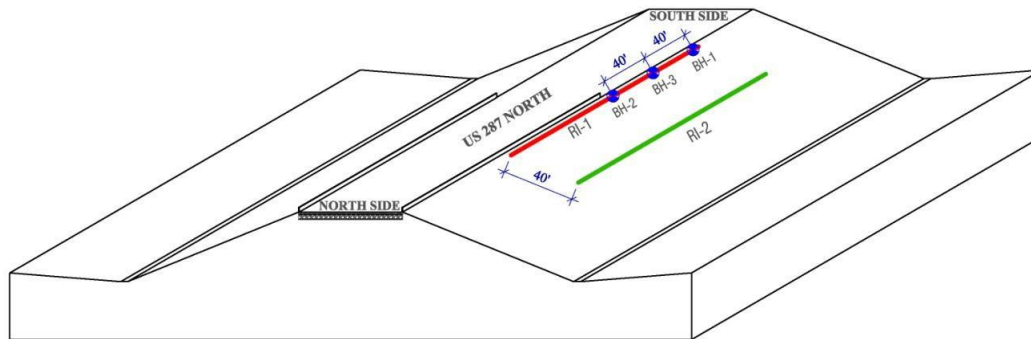
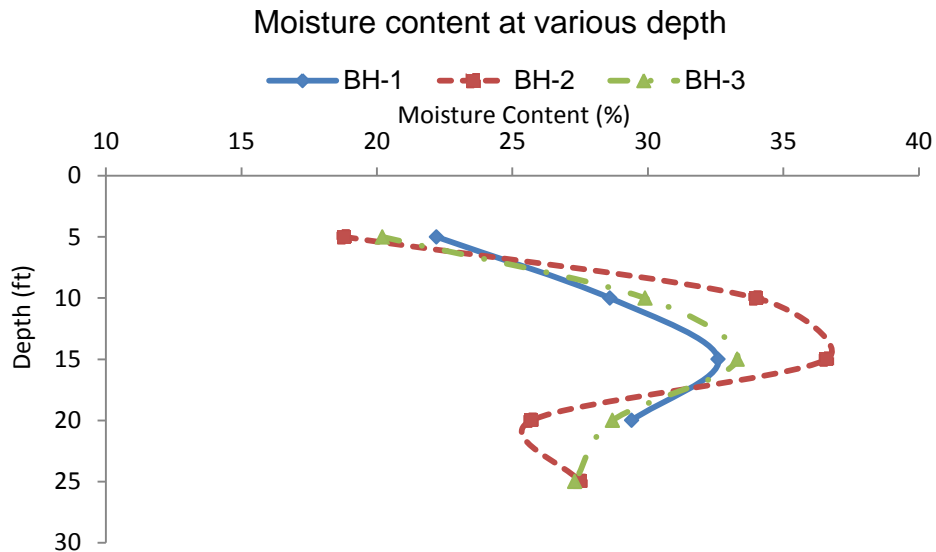


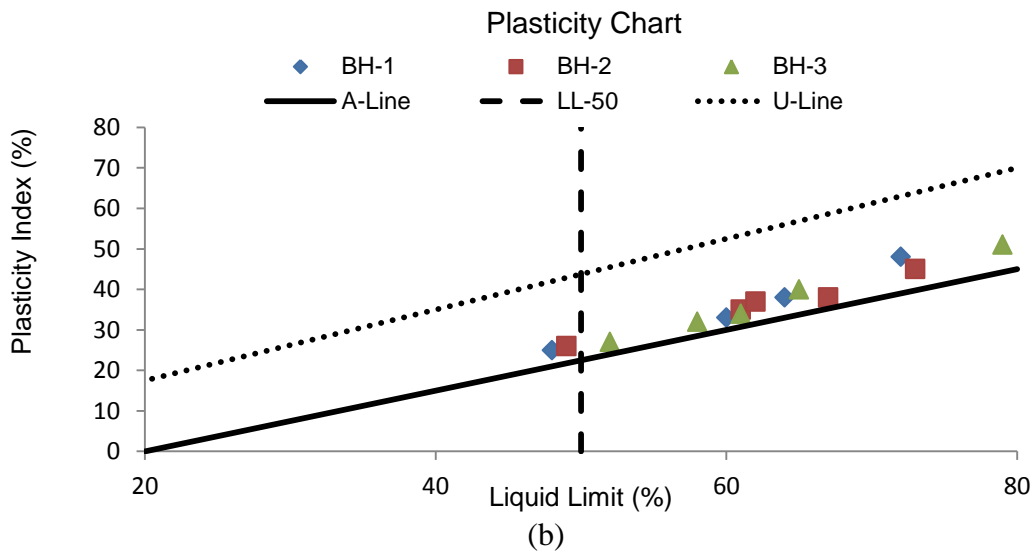
Figure 2-18 Borings and Resistivity Imaging location (Khan, 2013)

2.5.1.1 Geotechnical Boring and Laboratory Testing

A total of 3 soil test borings were performed near the crest of the slope. The depths of soil test boring ranged from 20 ft. - 25 ft. Both the disturbed and undisturbed soil samples were collected from different depths and tested to determine geotechnical properties of the subsoil. Based on the laboratory investigation results, all the collected soil samples were classified as high plastic clay (CH) soil according to the Unified Soil Classification System (USCS). The liquid limits and the plasticity indices of the samples ranged between 48-79 and 25-51, respectively. The moisture profiles on the depth and plasticity chart along the 3 bore holes are presented in Figure 2-19. The moisture profile indicated an increase in moisture below 5 ft. that ranged up to 20 ft.



(a)



(b)

Figure 2-19 Laboratory test results of US 287, (a) Moisture variation along the depth, (b)

Plasticity Chart of the soil in borings

2.5.1.2 Resistivity Imaging Profiles

2D resistivity imaging (RI) is extensively used in shallow geophysical

investigations and geo-hazard studies (Hossain et al., 2010). During the current study, the RI test was used to investigate the subsurface condition of US 287 slope. A total of two 2D RI lines, designated as RI-1 and RI-2, were conducted at the slope. RI -1 was conducted at the top of the slope near the crest, as presented in Figure 2-20. RI-2 was conducted at the middle of the slope, 40 feet. apart from RI-1.



Figure 2-20 Resistivity Imaging (a) RI-1 and (b) RI-2 at US 287

Geophysical investigations were conducted using 8-channel Super Sting equipment, which is relatively quicker than the conventional single channel unit. A total of 56 electrodes were used during the RI. The length of the each line was approximately 275 feet with electrode spacing of 5 feet c/c. The RI profiles along RI-1 and RI-2 are presented in Figures 2-21(a) and 2-21(b).

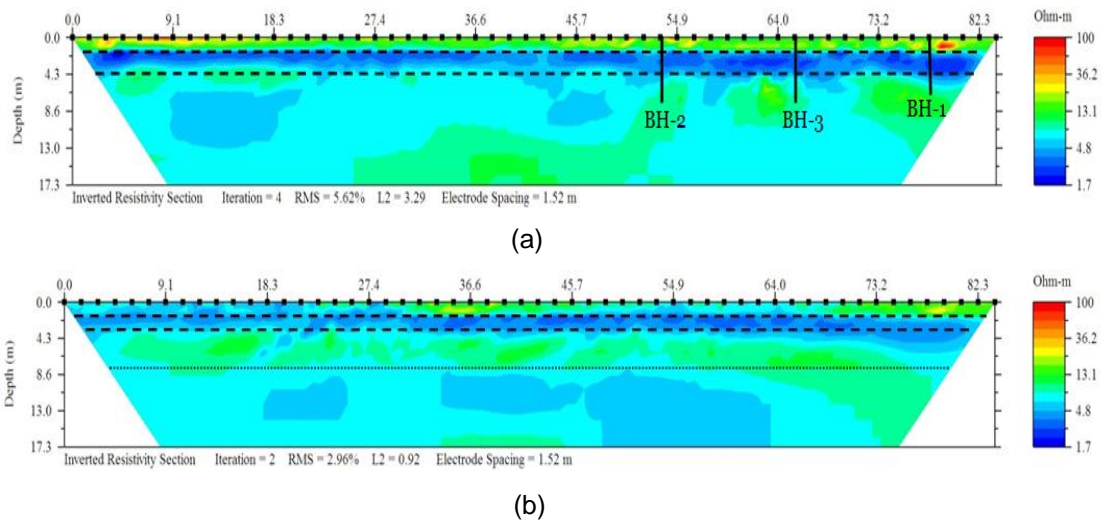


Figure 2-21 Resistivity Imaging Profile (a) Profile RI-1. (b) Profile RI-2

Based on the 2D RI profile, a low resistivity zone was observed near the top soil at both RI-1 (at crest) and RI-2 (middle of the slope). The resistivity of slope significantly decreased up to 16.4 ohm-ft. at depth from 5 ft. to 14 ft. It should be noted that the significant low resistivity might have occurred due to the presence of high moisture in the soil.

2.5.2 Analyses of Site Investigation Results

The subsoil investigation results indicated that the US 287 Slope was constructed using high plastic clay. In addition, the dominant mineral of the soil is montmorillonite. The high plastic clay, with the presence of montmorillonite, makes it highly susceptible to swelling and shrinking upon wetting and drying. It should be noted that fully softened strengths are eventually developed in high plastic clays in field condition after being exposed to environmental conditions (i.e. shrink and swell, wetting - drying) and provide the governing strength for first-time slides in both excavated and fill slopes (Saleh and Wright, 1997). The reduction in friction angle is not significantly due to cyclic wetting and drying of soil; however, the cohesion of the soil almost disappears in

the fully softened state (Saleh and Wright, 1997). The near surface soil at the US 287 slope may have been softened due to shrinkage and swell behavior which led to the initiation of movement of slope and resulted the crack over the shoulder.

Based on the subsoil investigation and resistivity imaging, it was evident that a high moisture zone existed between 5 ft. and 14 ft. near the crest of the slope. The shoulder crack provided easy passage of rain water into the slope which eventually led to saturation of soil near the crest. As a result, the driving forces increased, which decreased the factor of safety. It should be noted that the US287 slope did not failed during the investigation. However, the slope might fail within the next few years, as the movement initiated at the crest which is an indication of initiation of failure. A back analysis was performed, using the finite element method, to evaluate the critical shear strength at factor of safety equal to 1.0.

2.5.3 Slope Stability Analyses at US 287 Slope

Slope stability analysis by the elasto-plastic finite element method (FEM) is accurate, robust and simple. In addition, the graphical presentation of the FEM program allows better understanding of the failure mechanism. During this study, the slope stability analyses were performed using the FEM program, PLAXIS. The elastic perfectly plastic Mohr-Coulomb soil model was utilized for stability analyses using 15 node triangular elements. The 15-node element provides a fourth order interpolation for displacements and numerical integration that involves twelve stress points. The 15-node triangle is a very accurate element and has produced high quality stress results for different problems. Standard fixities were applied as a boundary condition, where the two vertical boundaries were free to move vertically and were considered fixed in the horizontal direction. The bottom boundary was modeled as fixed boundary.

During the slope stability analyses, it was considered that the initiation of

movement of the slope was going to take place with limiting FS equal to 1.0. To evaluate the soil parameters during the initiation of slope movement, back analyses were performed, using PLAXIS 2D. The shear strength reduction method (phi-C reduction analysis) was utilized to determine the factor of safety (FS). The factor of safety of a soil slope is defined as the factor by which original shear strength parameters can be reduced in order to reach the slope to the point of failure in shear strength reduction method.

The soil profile for the model is presented in Figure 2-22 (a). The top 7 ft. of soil was considered as failure zone, with a fully softened strength. Other soil parameters for different soil layers were utilized from field investigation results. Several iterations were performed during numerical analyses to evaluate soil parameters at failure. The soil parameters observed at failure from numerical modeling are presented in Table 277. Based on the FE analysis, the factor of safety was found to be 1.05, as presented in Figure 2-22 (b).

Table 2-7 Soil Parameters used in Plaxis

Soil Type	Friction Angle	Cohesion (psf)	Unit Weight (pcf)	Elastic Modulus (psf)	Poisson Ratio
1	10	100	125	100000	0.35
2	23	100	125	150000	0.3
3	15	250	130	200000	0.25
4	35	3000	140	250000	0.2

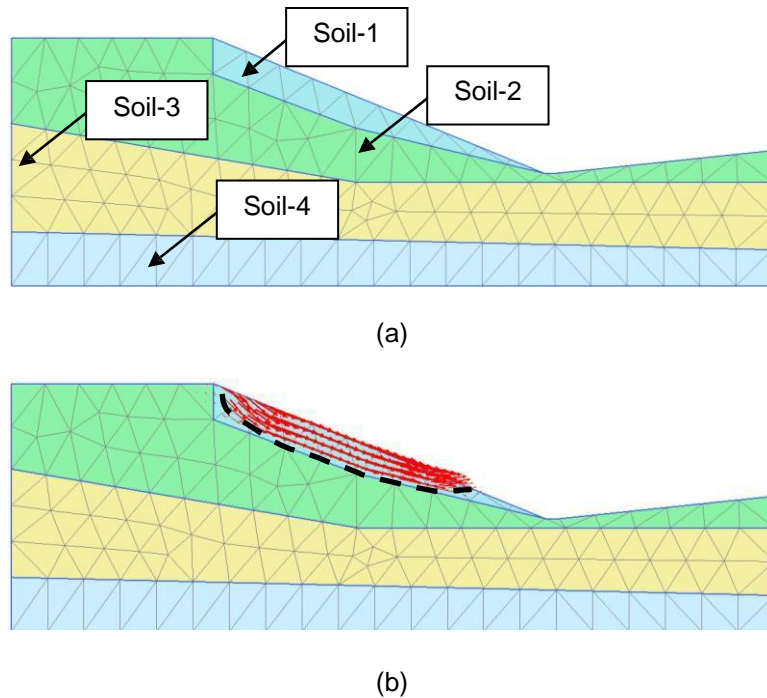


Figure 2-22 Slope stability analysis using Plaxis, (a) Soil Model , (b) Critical slip surface
(FOS 1.05) (Khan, 2013)

The FEM analysis indicated the typical failure pattern of shallow slope failure, which resembled the observed displacement trend at the US 287 slope. To resist any further failure of the slope, it was essential to take remedial action.

Three sections over the US 287 slope, designated as Reinforced Section 1, Reinforced Section 2 and Reinforced Section 3 were stabilized. In addition, two unreinforced control section (Control Section and Control Section 2) was considered between the reinforced sections to evaluate the performance of the reinforced section. The width of each section was 50 ft. The layout and cross section at each of the sections are presented in Figure 2-23 and 2-24, respectively.

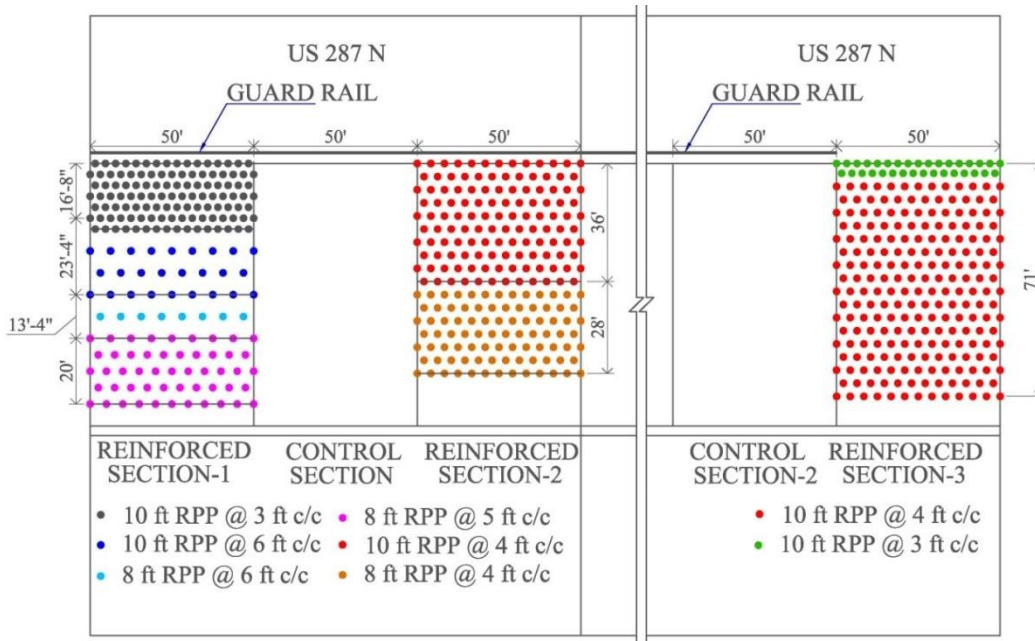


Figure 2-23 RPP layout at US 287 slope (Khan, 2013)

A combination of different lengths and spacing of RPP was considered for Reinforced Section 1. RPP at uniform spacing was considered for Reinforced Section 2 and Reinforced Section 3. 10 ft. long RPP at 3 ft.c/c spacing was considered near the crest of the slope at Reinforced Section 1. On the other hand, 6 ft. c/c spacing of RPP was taken into account at the middle of the Reinforced Section 1. Near the toe, 5 ft.c/c spacing was proposed, with 10 ft. length of RPP.

Different lengths of RPP (10 ft. at the crest and 8 ft. near the toe) were considered at Reinforced Section 2; whereas, Reinforced Section 3 was considered with constant length of RPP (10 ft.) throughout the entire slope. During this current study, RPP spacing of 4 ft. c/c was utilized for both Reinforced Section 2 and Reinforced Section 3. However, the first 2 rows of RPP at the crest of Reinforced section 3 were considered with 3 ft. c/c spacing. In addition, the first 2 rows should be installed below a 2 ft. depth from

the existing slope surface. RPP was considered to be placed in a staggered grid over the reinforced sections.

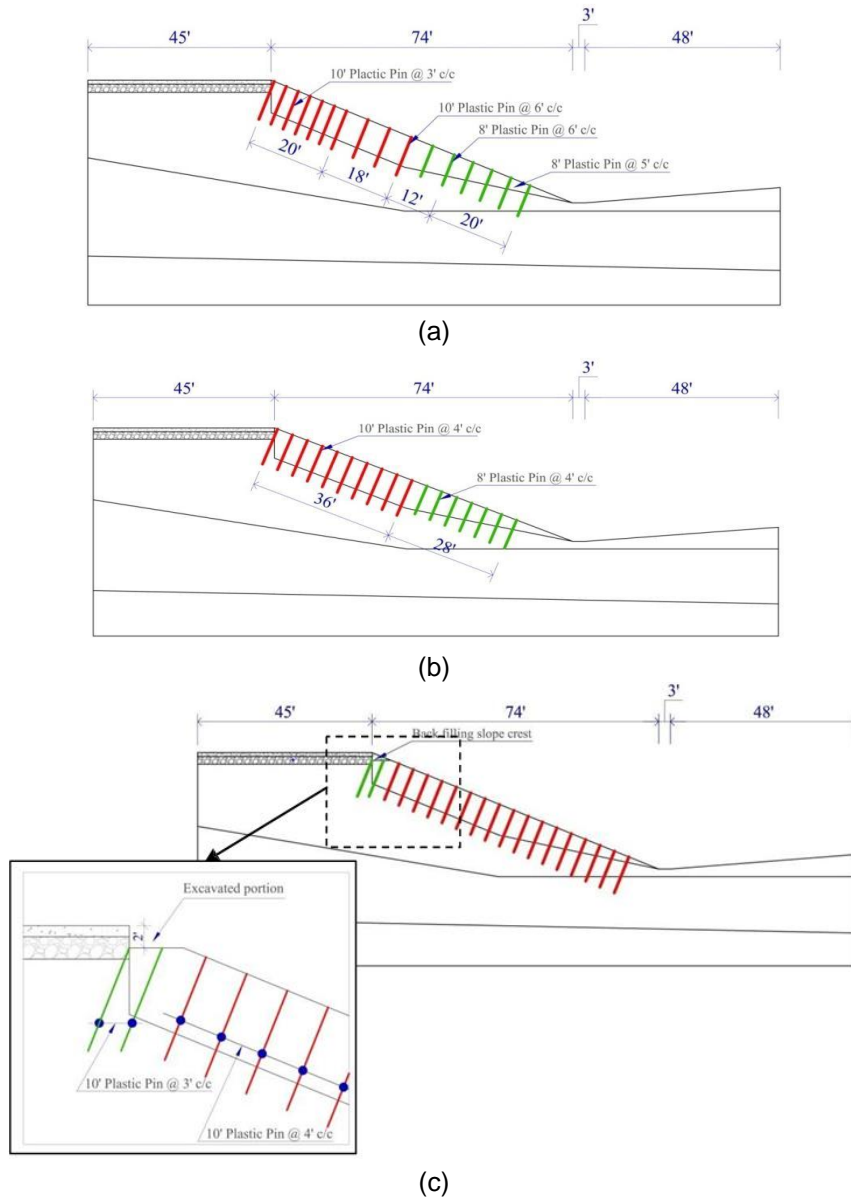
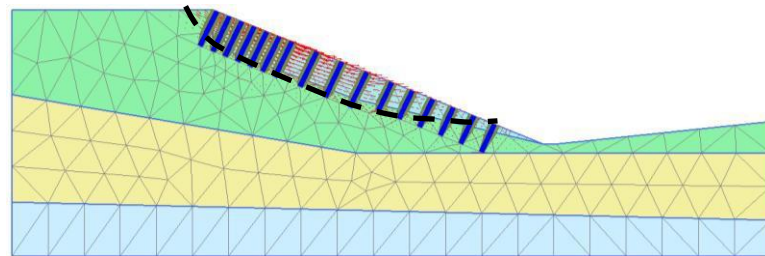
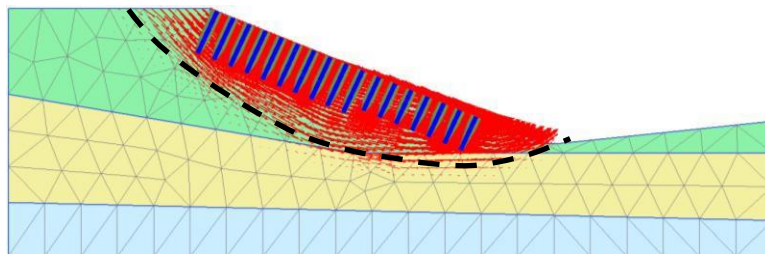


Figure 2-24 Section details of slope stabilization on US 287 Slope, (a) Reinforced section 1, (b) Reinforced section 2, (c) Reinforced section 3 (Khan, 2013)

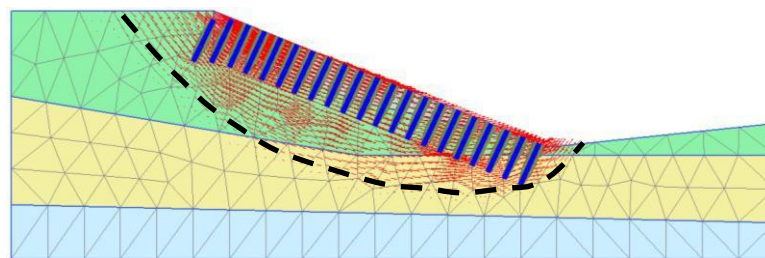
Based on the proposed distribution of RPP, the slope stability analyses were further conducted to evaluate the factor of safety of each reinforced section. The factor of safety was observed as 1.43, 1.48 and 1.54 for the Reinforced Section 1, Reinforced Section 2 and Reinforced Section 3 respectively. The critical slip surfaces for each of the reinforced sections are presented in Figure 2-25.



(a)



(b)



(c)

Figure 2-25 Slope stability analyses using RPP (a) Reinforced section 1 with FS 1.43, (b) Reinforced section 2 with FS 1.48 (c) Reinforced section 3 with FS 1.54 (Khan, 2013)

2.5.4 RPP instillation at US 287 Slope

Mast-mounted pseudo vibratory hammer system was used to install the RPP. The mast-mounted system maintains the alignment of the hammer and restricts imposing additional lateral loads during the RPP instillation (Bowders et al., 2003). Track rig is more suitable for the instillation over the slope, since no additional anchorage is required to maintain the stability of the rig and also reduce the instillation time resulting in cost reduction. The RPP instillation photos of US 287 slope are presented in Figure 2-26.



Figure 2-26 RPP instillation photo at US 287, (a) RPP instillation at Reinforced section 1, (b) RPP instillation at Reinforced section 2

In addition, benefit of using the mask-mounted rig with pseudo vibratory hammer is that the alignment of the pin with the hammer is always maintained during the installation. Hence the efficiency of the machine increases as the impact load from the pseudo vibratory hammer is transferred in the pin and it helps to penetrate the pin into the ground.

The RPP driving time was measured during the installation process. Based on the measured driving time, the average installation time, as well as the driving rate, is summarized in Table 2-8. It should be noted that the installation time per RPP is the summation of the time required to install and to maneuver the rig to the next location.

Table 2-8 Average RPP driving time at US 287 (Khan, 2013)

Location of RPP	Length of RPP (ft.)	RPP Spacing (ft.)	Average RPP Driving Time (min)	Average RPP Driving Rate (ft./min)
Reinforced Section 1	10	3	3.55	2.9
	10	6	4.76	2.1
	8	6	3.65	2.2
	8	5	2.63	3.1
Reinforced Section 2	10	4	2.76	3.6
	8	4	3.08	2.6
Reinforced Section 3	10	4	4.65	2.1

At Reinforced Section 1, the driving rate was observed as 2.85 ft/min. at 3 ft. c/c spacing for 10 ft. long RPP. The driving rate reduced to 2 ft/min. along the middle of the slope, with increase in RPP spacing of 6 ft. c/c. The reduction in driving rate was observed due to the longer maneuver time to shift equipment between higher spacing of RPP. Conversely, the highest driving rate of 3 ft/min. was observed near the toe of the Reinforced Section 1. The soil near the toe of the Reinforced Section 1 was very soft during the installation process. As a result, the installation time to drive RPP into the slope was reduced drastically, resulting in the highest driving rate. The overall average driving rate for Reinforced Section 1 was observed as 2.72 ft/min.

The driving rate was observed as 3.6 ft./min. at the top of Reinforced Section 2, where the RPP spacing was 4 ft. c/c. The driving rate was higher than the Reinforced Section 1, as the installation team became more efficient with the installation process. The driving rate was 2.6 ft./min. near the toe of Reinforced Section 2. It was lower due to

the existence of a stiff foundation layer at that location. The overall driving rate at Reinforced Section 2 was observed as 3.18 ft/min.

The installation in Reinforced Section 3 was conducted in the following year that had similar RPP spacing as Reinforced Section 2. However, a lower driving rate of 2.13 ft./min at Reinforce Section 3 was observed compared to the Reinforced Section 2. It should be noted that a new team installed the RPPs in Reinforced Section 3. Moreover, the RPP experienced a stiff foundation soil after a 7 ft. depth from the surface, which resulted in a higher installation time. The installation process was also delayed due to some driving equipment mechanical problems. As a result, the driving rate was low at the Reinforced Section 3.

Based on the study, the average driving rate, considering all three reinforced sections, was 2.66 ft/min., which signified that a 10 ft. long RPP could be installed within 4 min. Therefore, on average, a total of 100 to 120 numbers of RPPs could be installed within a day.

2.5.5 Performance Monitoring at US 287 Slope

Performance of the reinforced slope was monitored using the installation of inclinometers and a topographic survey on a monthly basis after installation of RPP. These results have been updated since the Khan, published in 2013.

2.5.5.1 Inclinometer

A total of 3 inclinometers, designated as Inclinnometer-1, Inclinometer 2 and Inclinometer 3, were installed at Reinforced Section-1, Control Section and Reinforced Section-2 to monitor the horizontal movement of the slope. The depth of each inclinometer casing was 30 ft., and they were installed perpendicular to the slope surface, 20 ft. below the crest. The layout of the inclinometers are presented in Figure 2-27

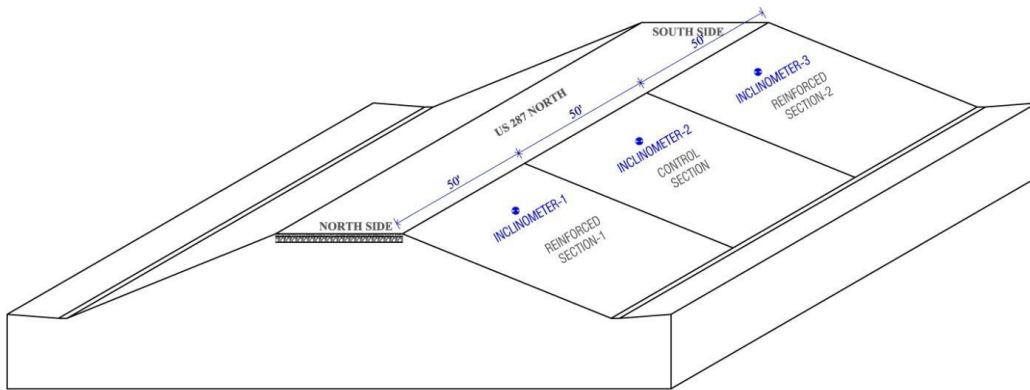


Figure 2-27 Layout of Inclinometer at US 287 slope

The inclinometers were monitored on a monthly basis, and the horizontal movement of Inclinometer 1 and Inclinometer 3 is included in the current study. Inclinometer 2 was blocked and was not included. The horizontal movement along with the moisture and suction variation are presented through Figures 2-28 and 2-29.

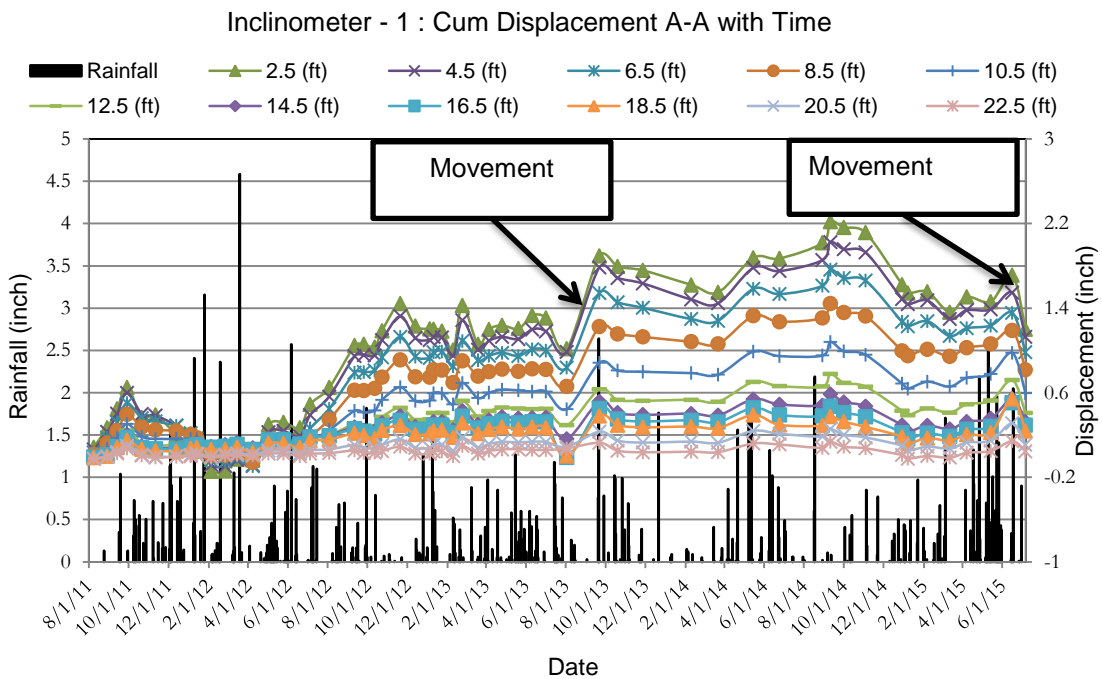


Figure 2-28 Displacement in Inclinometer I-1 at US 287

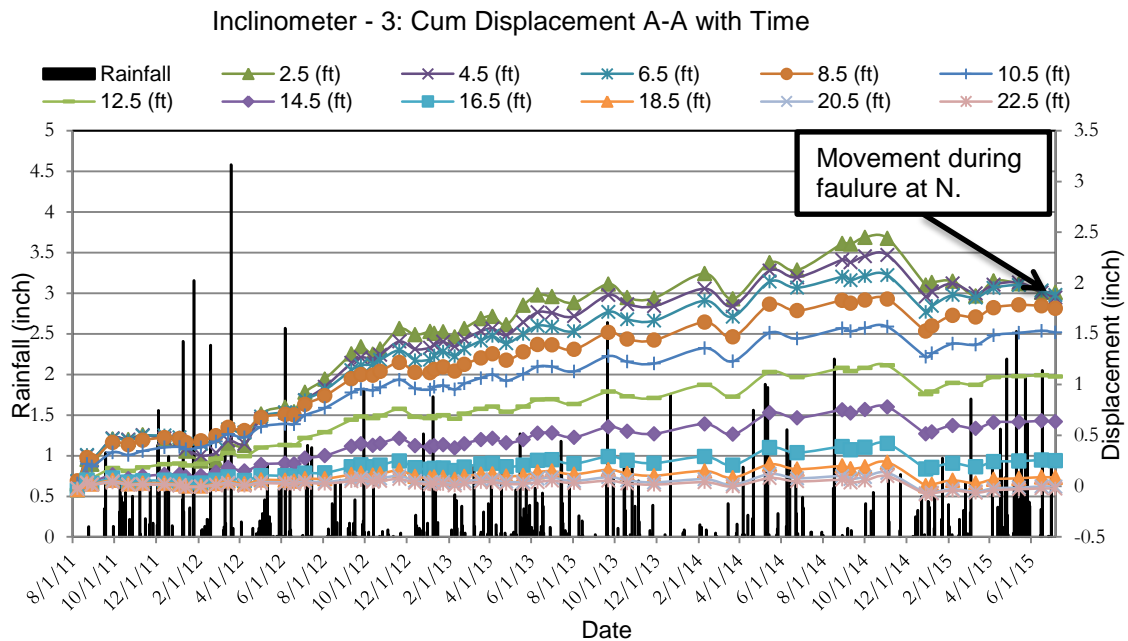


Figure 2-29 Displacement in Inclinometer I-3 at US 287

The US 287 slope had negligible movement during the wetting and drying period. The variations of horizontal displacement of the reinforced slope after October 2012 indicated that there was less than 0.1 inch movement in Inclinometer 1 (Reinforced Section 1) from October 2012 to June 2015. This is probably due to the fact that the load might have been mobilized in the Reinforced Section 1 and had less than 0.1 inch movement during the next wetting/drying period. There was an incremental horizontal displacement up to 0.5 inch during that period at Inclinometer 3 (Reinforced Section 2). The RPP was installed at the southbound slope.

On September 2013 there were slope failures at two locations over the south bound slope as shown in Figure 2-28. In addition, during the June 2015, two locations over the southbound slope had failed, due to a heavy rainfall event that month as shown in Figure 2-29. During the failure of the northbound slope, an increment in horizontal

displacement was observed at the reinforced section 1. However, no sign of failure was observed at the reinforced section.

2.5.5.2 Topographic Survey

A topographic survey was conducted over the US 287 slope as a part of the performance monitoring of slope stabilization. The first survey over the slope was conducted during May 2012, after the completion of RPP installation at Reinforced Section 3 and continued on monthly basis. During the survey, the cracked zones over the shoulder, as well as the RPP top at different reinforced sections, were monitored. The layout of the survey lines are presented in Figure 2-30.

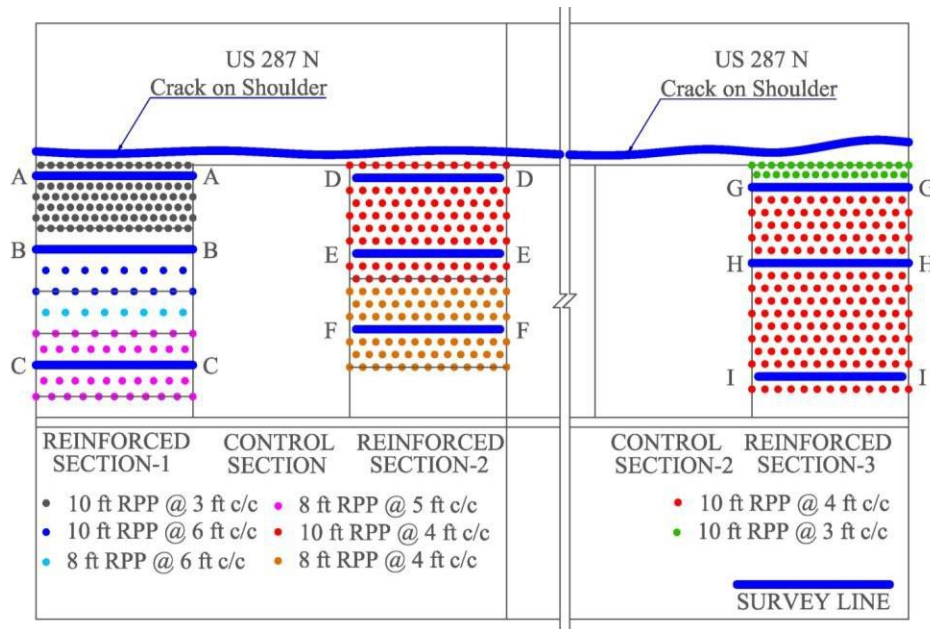


Figure 2-30 Layout of survey lines at US 287 slope

The total settlement over the crest of the slope was measured during each survey and presented in Figure 2-31. The total settlement plot presented that the control sections of the slope had significant settlement at the crest when compared to the reinforced sections. The maximum settlements were 16 inches and 10 inches in the

Control Section 1 and Control Section 2, respectively. On the other hand, the Reinforced Section 1 had the lowest settlement (3 inches) followed by the Reinforced Section 3 (5 inches) and Reinforced Section 2 (6 inches). It should be noted that the Reinforced Section 1 had the lowest spacing of RPP (3 ft. c/c) at the crest of the slope. Reinforced Section 2 and Reinforced Section 3 had 4 ft. c/c spacing at the crest, which was higher than Reinforced Section 1.

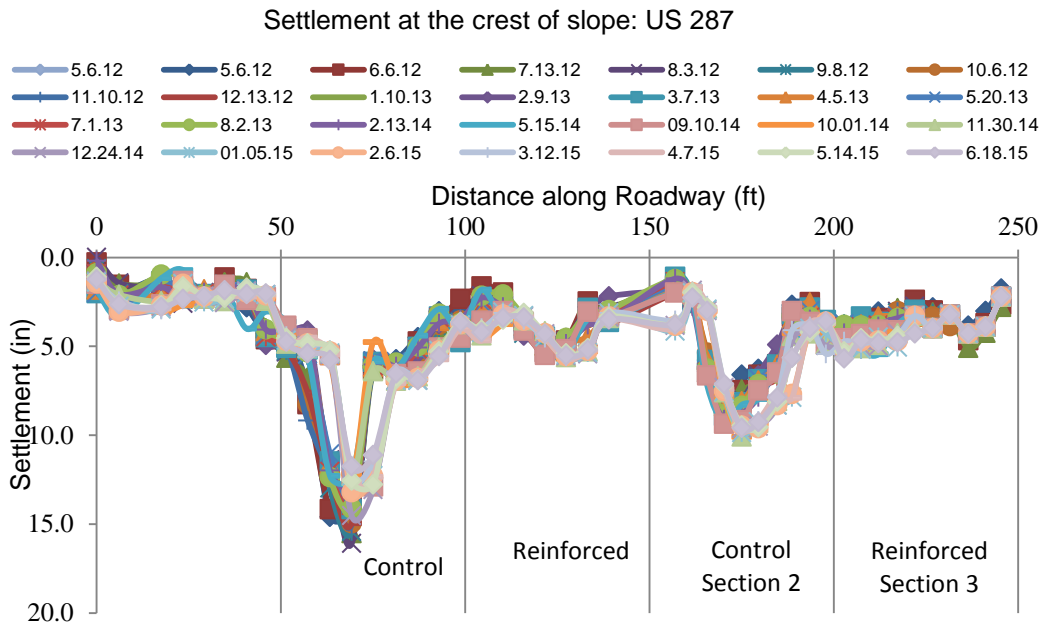


Figure 2-31 Settlement at the crest of the US 287 slope

Chapter 3

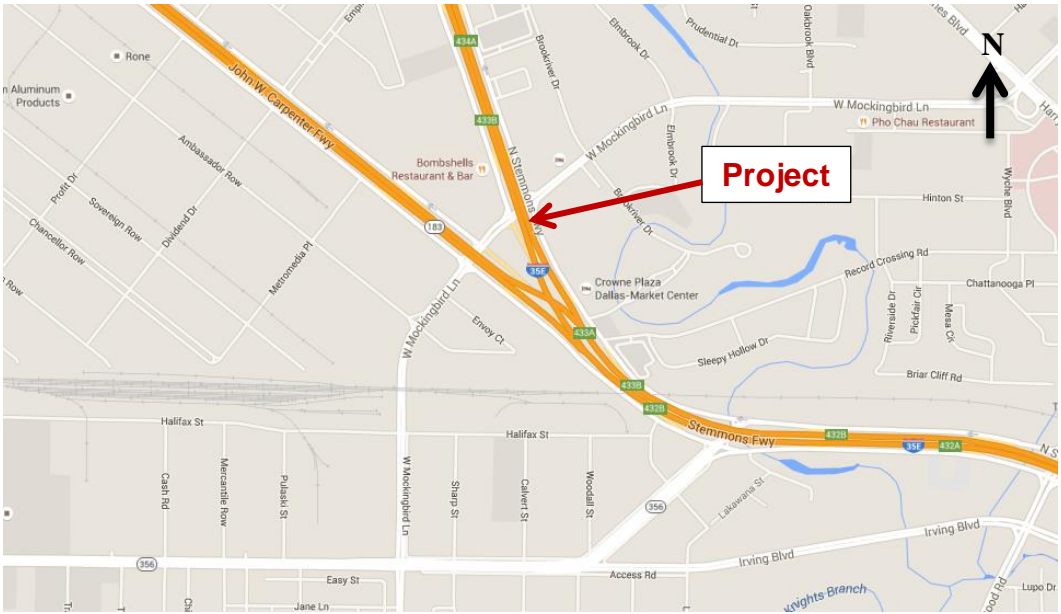
Site Investigation

3.1 Site Investigation Background

Generally, highway slope constructed with high plasticity clay is more susceptible to shrinkage and swelling behavior which results in shallow slope failures around Dallas Fort-Worth area. Therefore, three highway embankments were selected in this region for current study. First slope is located in State Highway (SH) 183 east and northbound SH 360 in the northeast corner of Tarrant County, Texas. Second slope is located at Interstate Highway I-35 and Mockingbird lane in Dallas. Surficial slope movement was observed in all three slopes. A site investigation program was conducted to investigate the cause of the movement of the slopes. The detail site investigation of each of these slope are presented in this chapter.

3.2 Site Investigation of I-35 and Mockingbird Slope

The Slope is located along north bound I-35E near the south of Mockingbird Lane overpass and the failure photos are as shown in Figure 3-1(a) and 3-1(b), respectively. Crack was observed over the shoulder due to the surficial movement at the slope. The crack propagated up to 42 ft. over the shoulder. The schematic of the failure condition are presented in Figures 3-2.



(a)



(b)

Figure 3-1 Project Information (a) Project location of I-35 slope, (b) Failure photos of I-35.

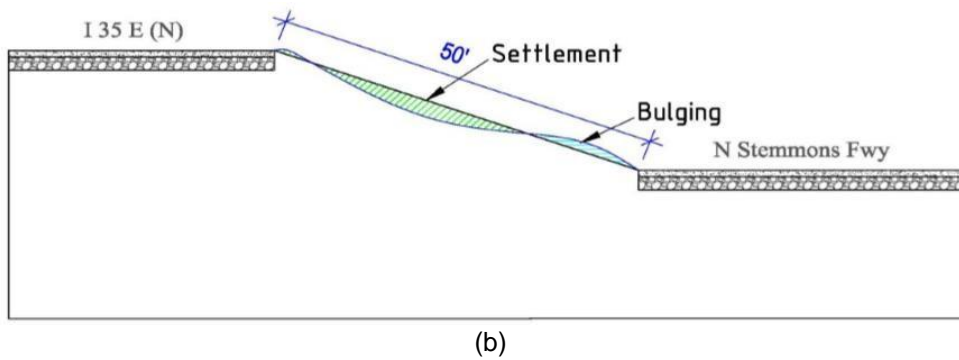
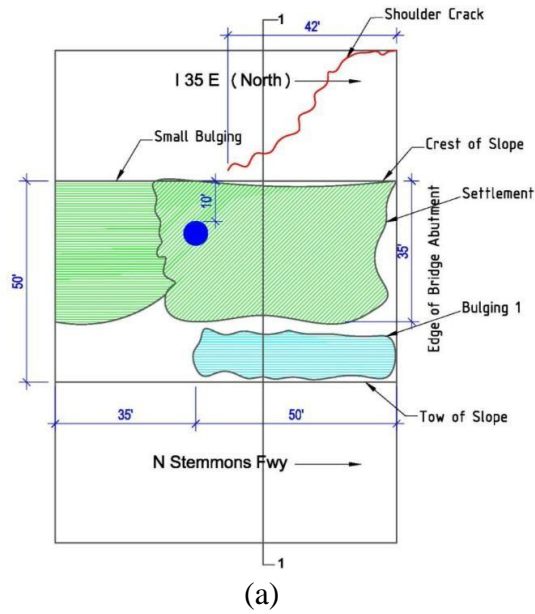


Figure 3-2 Schematic of the failure condition, (a) Front elevation view,
(b) Cross-section 1-1

3.2.1 Site Investigation I-35

The site investigation of the Mockingbird site was performed on February 2014. The site investigation program included geophysical testing using resistivity imaging (RI) and soil test borings. The layout of the RI test lines and soil test borings are presented in Figure 3-3

3.2.2 Geotechnical Borings and Laboratory Testing

A total of three soil test borings were conducted on February, 2014 in the Mockingbird slope. Borings locations are presented in Figure 3-3. The soil boring BH-1 was located over the crest of the slope. On the other hand, the BH-2 and BH-3 were located near the toe of the slope. The depth of each of the test boring was 30 ft. Both disturbed and undisturbed samples were collected from the borings. The disturbed samples were collected during the time of auger boring. The collected soil samples were tested in the laboratory for use in the design.

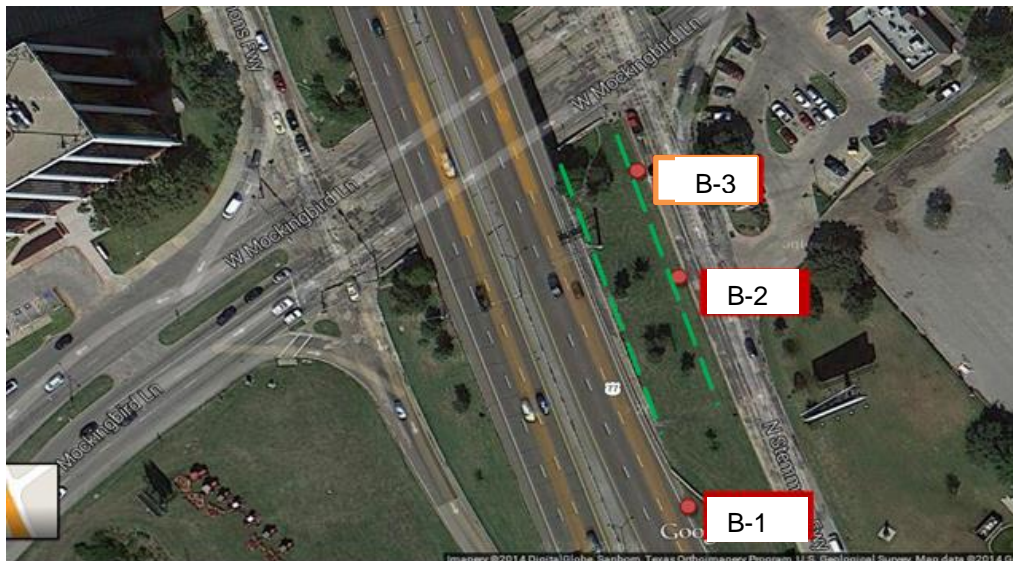


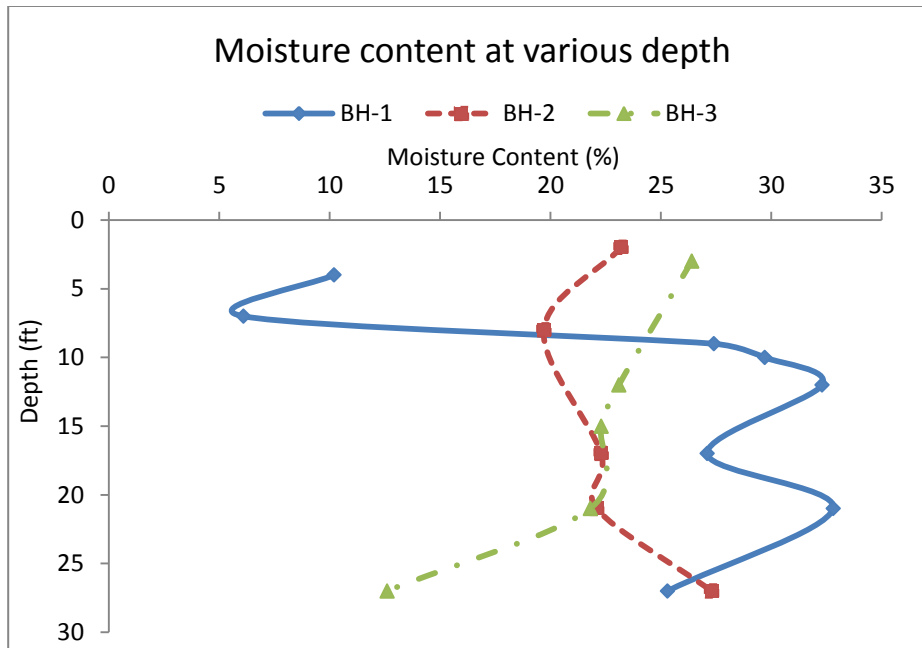
Figure 3-3 Borings and Resistivity Imaging location at I-35

The soil test borings and laboratory test results are presented in Table 3-1 and also plotted in Figure 3-4. The presence of high moisture zone was observed between 10 and 30 feet based on the laboratory investigation done on samples taken from Boring BH-1. The high moisture zone from BH-1 was in good agreement with the resistivity profile below the failure zone.

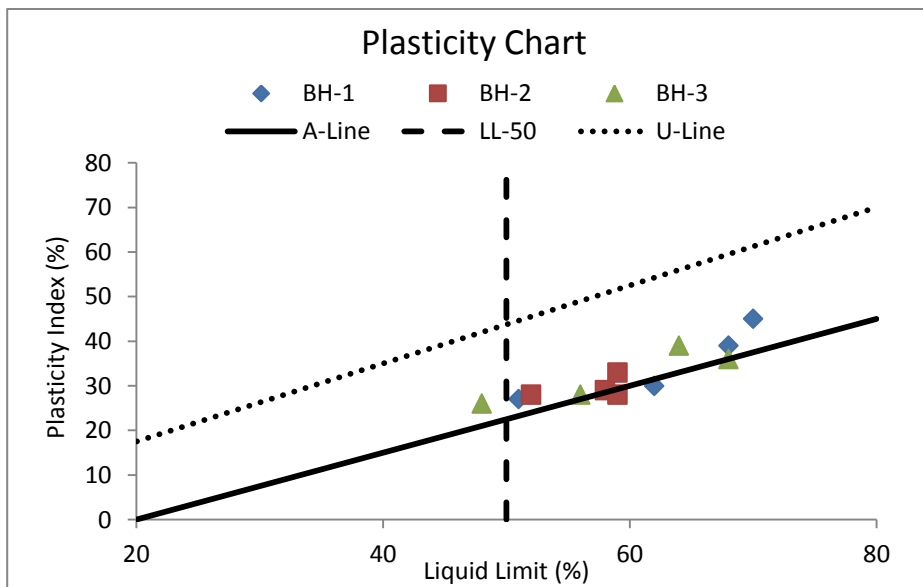
The soil boring results presented that the soil type is high plastic clayey soil. Usually, the shear strength of the high plastic clay soil softened within the few years after construction due to the shrinkage and swelling behavior. Moreover, the shrinkage crack acts as a conduit for rain water intrusion and possibly saturates the top of slope. The infiltrated rain water might saturate the top soil and might cause the failure of the slope.

Table 3-1 Soil test results of I-35

Boring	Depth (ft)	Liquid Limit (%)	Plasticity Index (%)	Moisture Content (%)	Soil Type
BH-1	4	-	-	10.2	-
	7	51	27	6.1	CH
	9	-	-	27.4	-
	10	62	30	29.7	CH
	12	-	-	32.3	-
	17	68	39	27.1	CH
	21	-	-	32.8	-
	27	70	45	25.3	CH
BH-2	2	52	28	23.2	CH
	8	58	29	19.7	CH
	17	-	-	22.3	-
	21	59	28	22.1	CH
	27	59	33	27.3	CH
BH-3	3	68	36	26.4	CH
	12	64	39	23.1	CH
	15	-	-	22.3	-
	21	48	26	21.8	CL
	27	56	28	12.6	CH



(a)



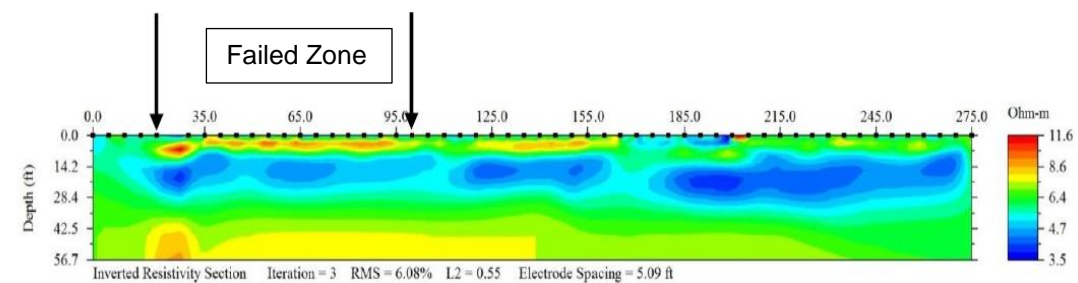
(b)

Figure 3-4 Laboratory test results of I-35, (a) Moisture variation along the depth, (b) Plasticity chart of the soil in borings

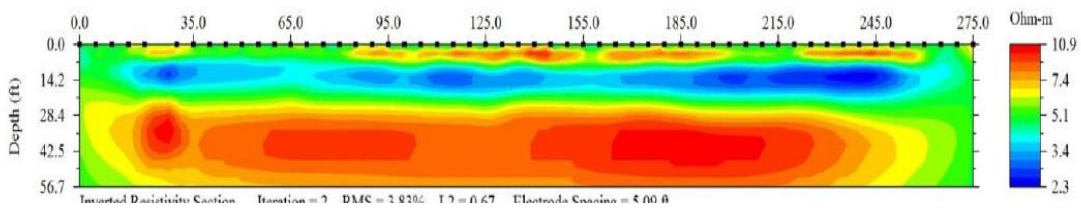
3.2.3 Resistivity Imaging

A total of two 2D resistivity imaging lines were conducted at the site. The 2D imaging sections are identified as RI-1 and RI-2 are presented in Figure 3-5. Resistivity Lines RI-1 and RI-2 were located near the crest of the slope and near the toe of the slope, respectively.

The resistivity profile for RI-1 indicated that there was a high resistivity zone at the surface of the slope at the failure area. The depth of the high resistivity zone was observed as 7 feet. It should be noted that during the surficial soil movement, the failure zone might have become loose and/or disturbed which might have caused the high resistivity zone. Therefore, depth of failure due to the surficial soil movement could be as much as 7 feet. A low resistivity zone was observed immediately below the failure zone. The low resistivity might signify the presence of high moisture zone under the failure area.



(a)



(b)

Figure 3-5 Resistivity Imaging results of I-35 slope, (a) RI-1 and (b) RI-2

3.2.4 Slope Stability Analysis and Design of Slope Reinforcement

Slope stability analyses were performed using Finite Element program PLAXIS. The general Mohr-Coulomb soil model was used for the stability analyses. Two different soil layers were identified during filed investigation. Modeling was performed using the fully softened shear strength of the soil for the top soil. Soil strength beyond the failure zone was not reduced for the analysis. Soil parameters used for the analyses are presented in Table 3-2

Table 3-2 Soil parameters used for slope at I-35

Material	γ (lb/ft ³)	c (psf)	Φ (degrees)	E (lb/ft ²)	v
Top Soil	125	40	17	15500	0.35
Bottom Soil	130	250	20	200000	0.3

The stability analysis of the unreinforced slope indicated that the factor of safety was 1.03 which is very close to the failure. The failure plane is presented in Figure 3-6.

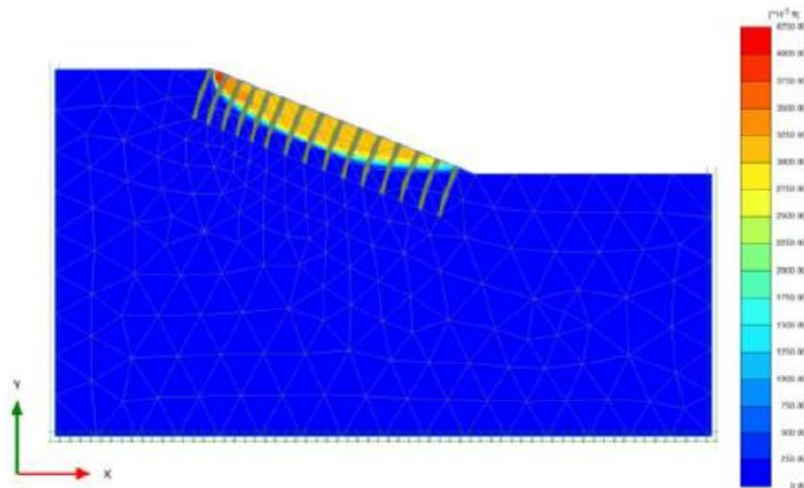


Figure 3-6 Slope stability of I-35 slope using Plaxis (FOS 1.03)

3.3 Site Investigation of SH 183 Slope

3.3.1 Project Background

The slope is located along SH 183 east of the exit ramp from eastbound SH 183 to northbound SH 360 in the northeast corner of Tarrant County of TxDOT's Fort Worth District as shown in Figure 3-7. Surficial failure and bulging occurred near the crest of the slope. The schematic of the failure condition and failure photos are presented in Figures 3-8 and 3-9, respectively.

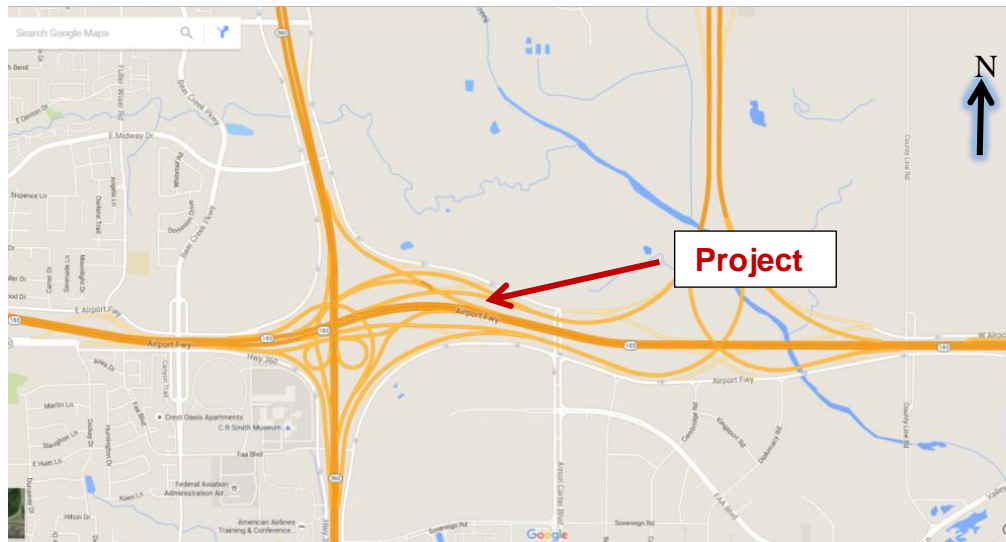
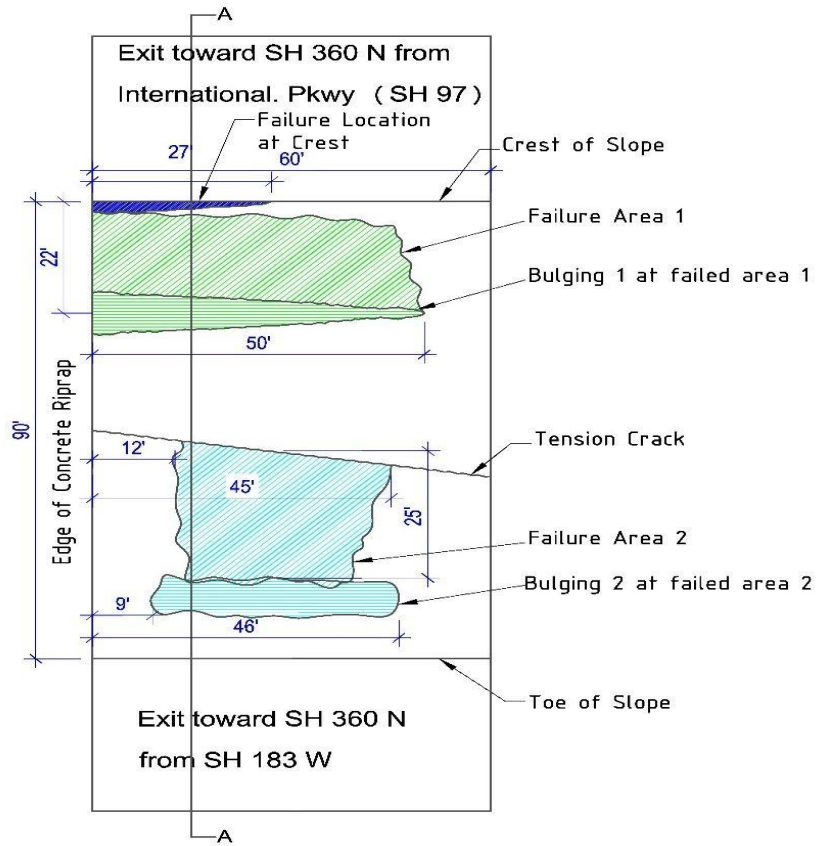
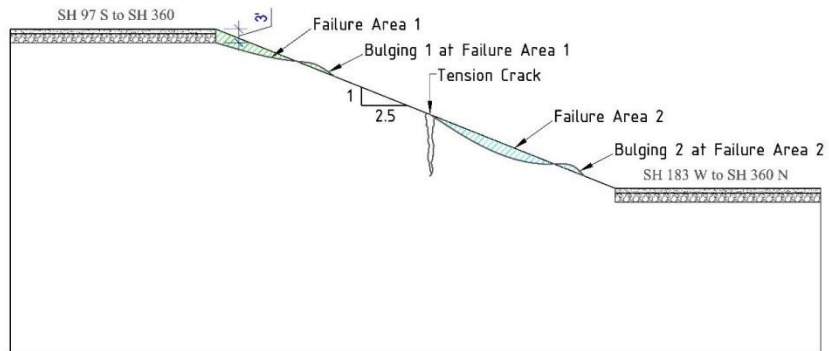


Figure 3-7 Project location of SH 183



(a)



(b)

Figure 3-8 Schematic of the failure condition, (a) Front elevation view, (b) Section A-A



Figure 3-9 Slope failure photos at SH 183

3.3.2 Site Investigation SH 183

An extensive site investigation program was undertaken on the SH 183 slope location. The site investigation included soil sampling from test borings, laboratory testing of the collected soil samples and geophysical investigation using 2D RI. The layout of the soil test borings and RI lines are presented in Figure 3-10.



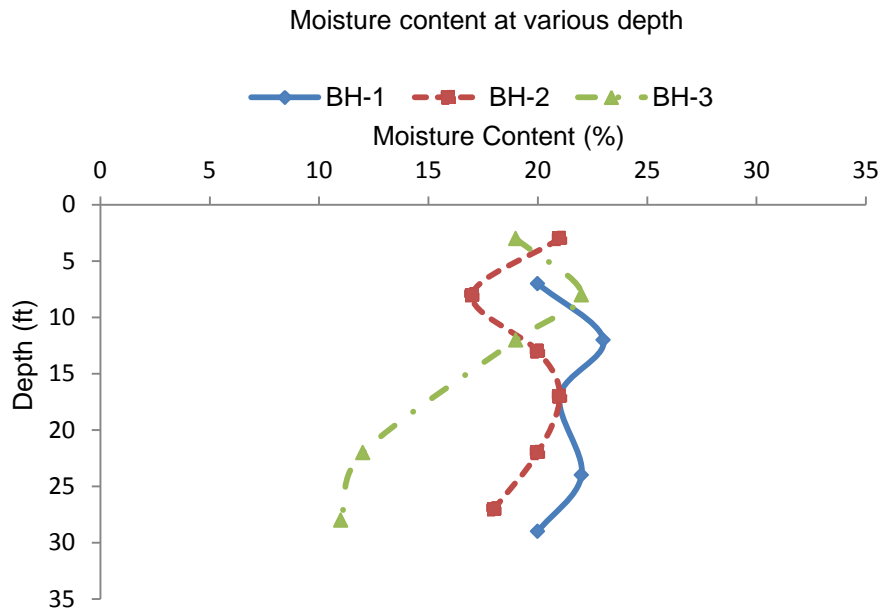
Figure 3-10 Borings and Resistivity Imaging location

3.3.3 Geotechnical Boring and Laboratory Testing

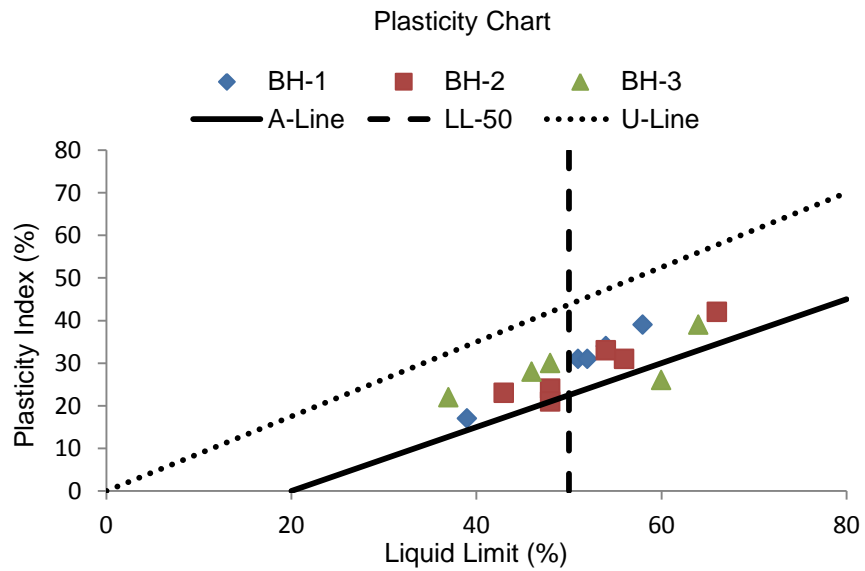
The liquid limit and the plasticity index of the soil samples from each borehole were determined and are summarized in Table 3-4. Based on the soil test results, the soil samples were classified as low to highly plastic clay according to the Unified Soil Classification System (USCS). Soil in the top layer from Boreholes BH-1 and BH-2 was classified as low plastic clay (CL). Soil in the top layer from Borehole BH-3 was classified as high plastic clay (CH). A possible explanation of this reversal might be due to the pavement subgrade soil at Boreholes BH-1 and BH-2 as they were drilled through the pavement along the roadway shoulder at the crest of the slope where one of the failures occurred.

Table 3-3 Soil test results of SH 183

Boring	Sample Depth (ft)	Liquid Limit (%)	Plasticity Index (%)	Moisture Content (%)	Soil Type
BH-1	7	39	17	20	CL
	12	51	31	23	CH
	17	58	39	21	CH
	24	52	31	22	CH
	29	54	34	20	CH
BH-2	3	43	23	21	CL
	8	48	24	17	CL
	13	66	42	20	CH
	17	56	31	21	CH
	22	54	33	20	CH
BH-3	27	48	21	18	CL
	3	60	26	19	CH
	8	64	39	22	CH
	12	48	30	19	CL
	22	46	28	12	CL
	28	37	22	11	CL



(a)



(b)

Figure 3-11 Laboratory test results of SH-183, (a) Moisture variation along the depth, (b) Plasticity chart of the soil in borings

The variations of moisture content within the borehole vertical profiles and Plasticity Chart of the Borings are also presented in Figures 3-11(a) and 3-11(b), respectively. It was observed that moisture content of the soil samples collected from Boring BH-1 ranged from 20% to 23% after 5 ft. Moisture content was 17% to 21% for the soil collected from Boring BH-2. During the field visit, shoulder cracks were observed near the crest of the slope which may work as a potential pathway for the intrusion of rainwater. Once the rain water gets in to the slope, it sits there unless it dried up or percolated into the deeper layer. However, the percolation in the clay soil is usually take longer time due to the low permeability.

It should be noted that the high moisture zone below the pavement might take place due to intrusion of rain water through the shoulder crack. However, the low moisture content at the top of the BH-1 might be due to the presence of any possible anomaly in the pavement layer. In Boring BH-3, moisture content was higher at the top 5 ft. (around 20%) and gradually decreased with depth. The high moisture content at the top 5 ft. might indicate the formation of the perched water condition due to the intrusion of rain water and low permeability of the high plastic clay soil.

3.3.4 Resistivity Imaging

A total of 3 (three) 2D resistivity imaging (RI) lines were conducted at the site. The 2D imaging sections are identified as “Resistivity Line 1”, “Resistivity Line 2” and “Resistivity Line 3” and are presented in Figure 3-12. Resistivity Line 1, Resistivity Line 2 and Resistivity Line 3 were located near the crest of the slope, at the mid-height of the slope over the tension crack, and near the toe of the slope, respectively.

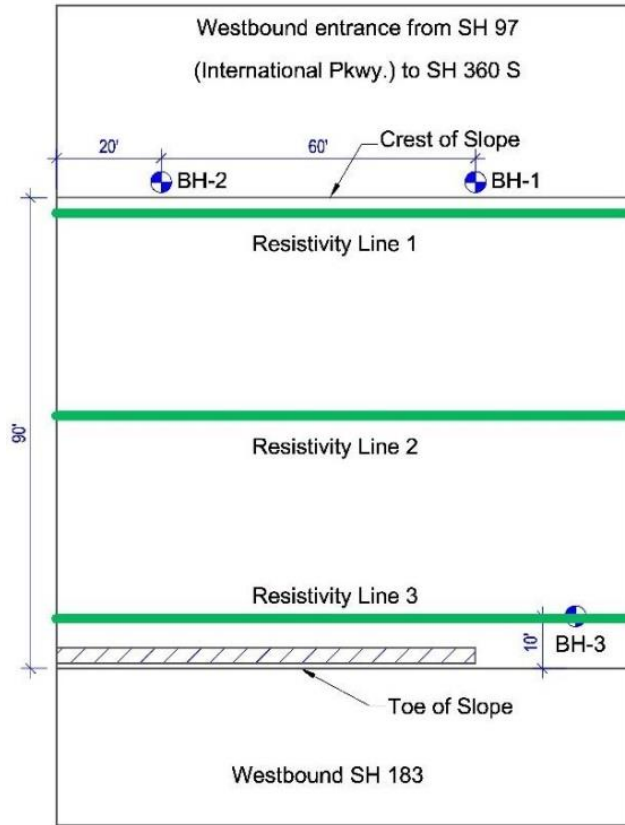


Figure 3-12 Location of Resistivity Imaging at SH 183

The RI investigations were conducted using an 8-channel Super Sting Resistivity meter with 56 electrodes. The electrodes were placed on a 5 feet spacing during each RI test to develop a profile for each line. The 2D profiles of the RI tests are presented in Figure 3-13.

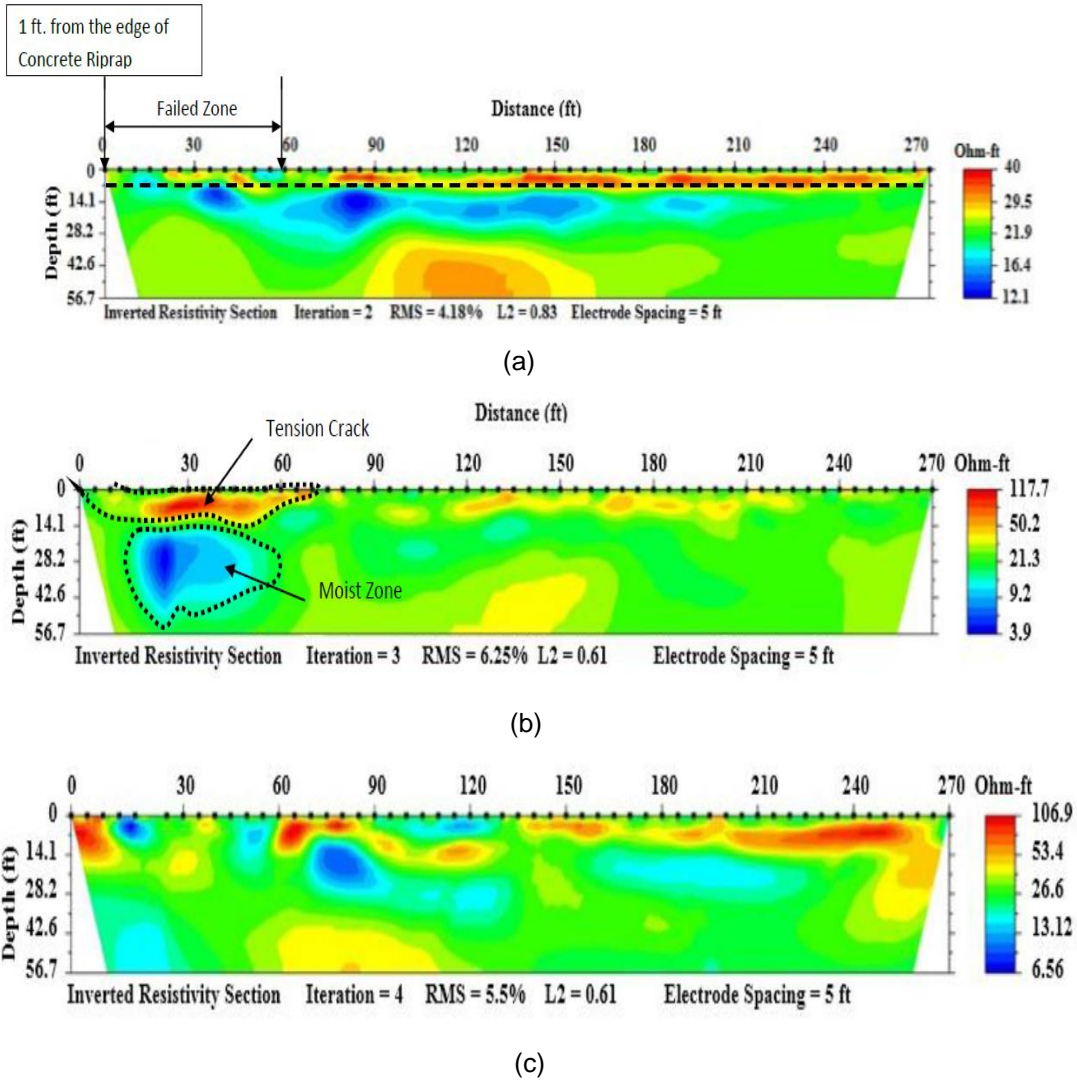


Figure 3-13 Resistivity Imaging profiles of SH 183, (a) RI Line 1, (b) RI Line 2, (c) RI Line 3

Based on the 2D RI profiles, a 7 ft. deep high resistivity zone was observed near the crest of the slope which might occur due to the disturbance during slope failure or the presence of the active zone. It should be noted that the resistivity of the soil depends on the soil type, moisture conditions and void ratio of the soil. Due to slope movement, the soils at the failed zone become loose which may result in higher void ratio and high

resistivity. In contrary, the presence of moisture results in the low resistivity of the soil. As presented in Figure 3-13 a high resistivity zone exist along the tension crack which may indicate the extent of the tension crack and a low resistivity zone that may indicated a moist zone due to the intruded rainwater through the tension crack. Based on Figure 3-13, the extent of the tension crack is up to 10 ft.

3.3.5 Shear Strength Test

The soil samples from different depths within each Borehole were further investigated to evaluate the peak, fully softened and residual shear strength of the soil. The peak shear strength of the undisturbed samples is summarized in Table 3-4. Besides, the peak fully softens shear strength and residual shear strengths of the remolded samples are presented in Table 3-5. The shear strength tests were further utilized to conduct slope stability analysis and design of the slope stabilization scheme.

Table 3-4 Shear Strength Test on Undisturbed Samples

Boring No.	Sample Depth (ft)	Specimen	Test Type	Cohesion (psf)	Friction Angle
BH-1	3	Undisturbed	Direct Shear	550	21
BH-2	19	Undisturbed	Direct Shear	500	13
BH-3	3	Undisturbed	Direct Shear	403	20
BH-3	15	Undisturbed	Consolidated Undrained Triaxial	610	12
BH-3	19	Undisturbed	Direct Shear	950	16

Table 3-5 Shear Strength Test on Remolded Samples

Boring No	Sample Depth (ft)	Specimen	Test Type	Cohesion (psf)	Friction Angle
BH-3	3	Remolded with Wet-Dry Cycle	Direct Shear	120	21
BH-3	3	Remolded	Ring Shear	142	26

3.3.6 Slope Stability Analysis

Slope stability analyses were performed using the Finite Element Modeling program PLAXIS using Mohr-Coulomb soil model. The general Mohr-Coulomb soil model was used for the stability analyses. Modeling was performed using the fully softened shear strength of the soil for the top 7 feet of soil, as a possible softened zone (disturbance) was observed at a depth of 7 feet during resistivity imaging. To simulate the fully softened layer, a new layer was introduced during the analysis considering the fully softened strength. The fully softened strength was utilized from the shear strength test results considering the wet-dry cycles. Soil strength beyond the failure zone was not reduced for the analysis. The Soil Slope model and soil properties are presented in Figure 3-14 and Table 36, respectively. The Factor of Safety (FS) obtained from the analyses was found to be 1.463.

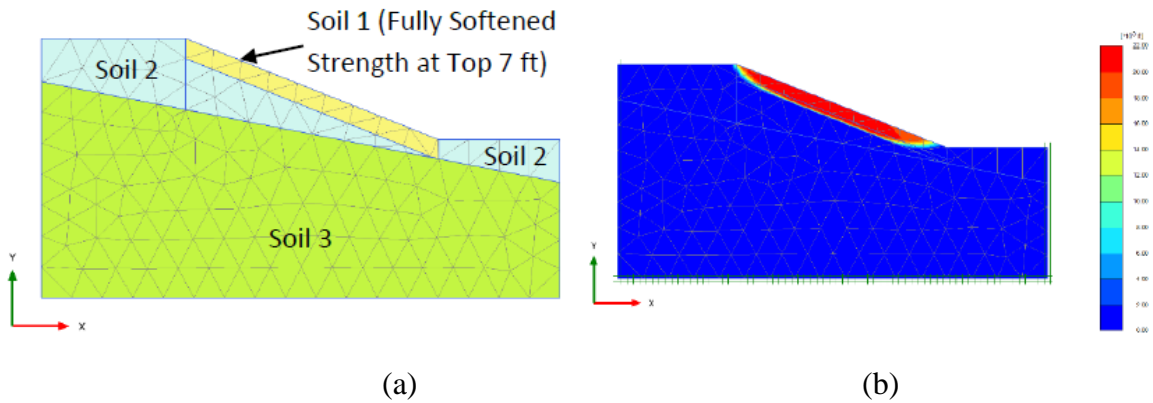


Figure 3-14 Slope stability analysis of SH 183 slope, (a) Soil Model, (b) Fully softened strength at top 7 ft. (FOS 1.463),

Table 3-6 Soil parameters used at SH 183

Soil Layer	Friction Angle	Cohesion (psf)	Unit Weight (pcf)	Elastic Modulus (ksf)	Poisson Ratio
1	20	120	125	100	0.35
2	21	400	19.6	100	0.3
3	20	950	16	200	0.25

The analyses were further continued considering a perched water zone (a fully moistened zone) formation due to rainfall. It is theorized that due to the seasonal wet-dry cycles, the high plastic CH clay contracted and created a path for the intrusion of rain water. The intruded rain water may saturate the top few feet of the soil and sit there may be for few days due to the low permeability of the high plastic clay soil and might form a temporary a perched water zone. During this analysis, the temporary perched water zone (fully moistened zone) was considered at 5 ft. The slope stability analysis result indicated

that the Factor of Safety may be reduced to almost 1.09 at a presence of 5 ft. perched water table from the top of the slope. The outputs from the slope stability analyses are also presented in Figures 3-15(a) and 3-15 (b).

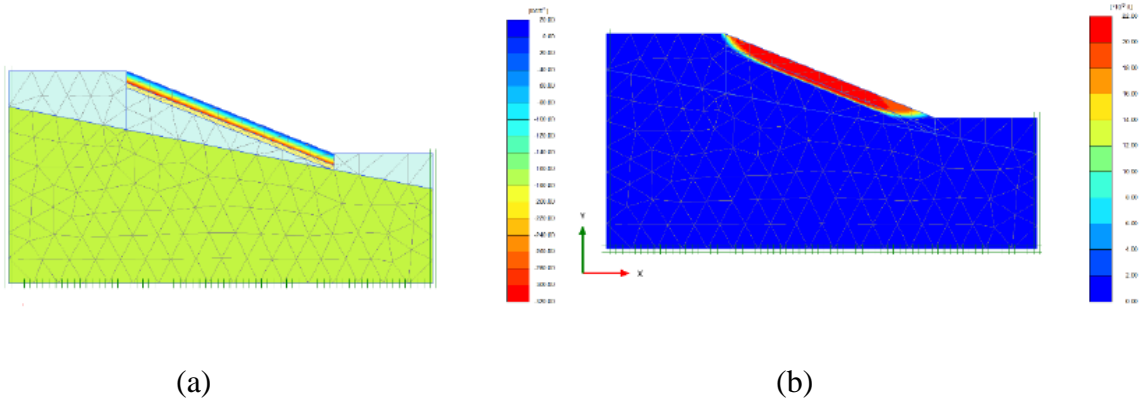


Figure 3-15 Slope stability analysis of SH 183, (a) Soil Model,
(b) Perched water at top 5 ft (FOS 1.098)

Chapter 4

RPP Instillation and Slope Monitoring

4.1 Slope Stabilization at I-35 Slope

Eighty five feet section of I-35 slope was considered to install the RPP and reinforced the slope. The slope stability analysis was further conducted considering 4 inch x 4 inch rectangular fiber reinforced RPP. The length of the RPP was considered as 10 ft. In addition, 6 rows of RPP near the crest of the slope were considered at a spacing of 3 ft. c/c. On the other hand, 5 ft. spacing of RPP was considered at the rest of the slope near the toe. The slope stability analyses was further continued to determine the factor of safety of the reinforced slope. The factor of safety of the reinforced slope was observed as 1.74. The proposed layout of the RPP for the Mockingbird slope is presented in Figure 4-1. The failure plane of the reinforced slope is also presented in Figure 4-2.

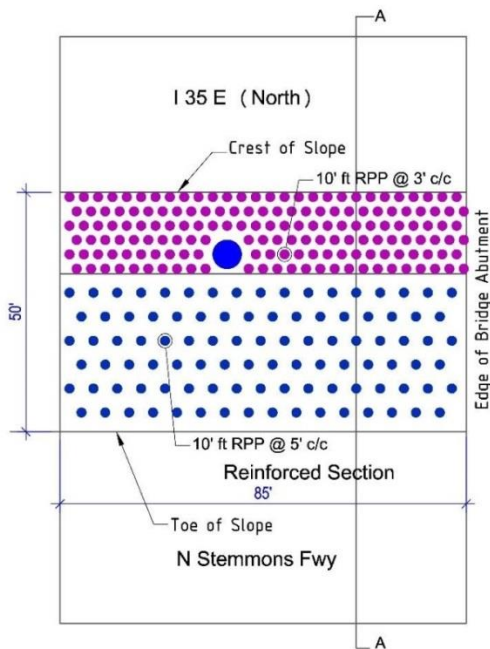


Figure 4-1 Proposed layout of the RPP for the Mockingbird slope

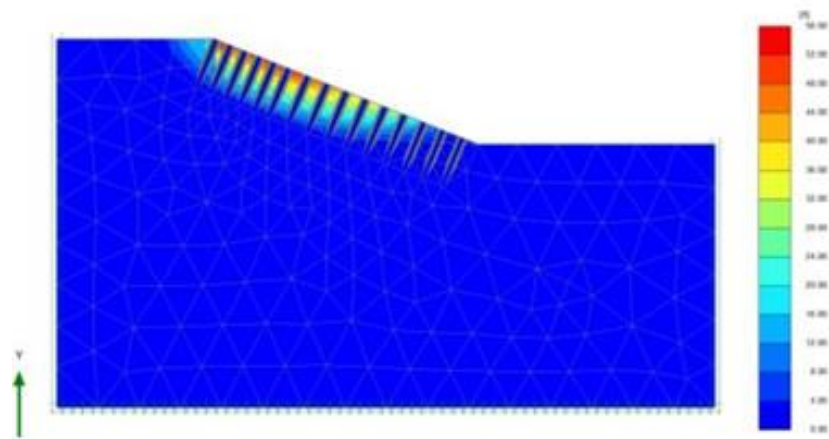


Figure 4-2 Slope stability analysis, FOS 1.74

4.2 RPP instillation at I-35 Slope

Field installation activities at Mockingbird slope started on middle of May 2014. Previous study indicated that the crawler mounted rig with an mast mounted pseudo vibratory hammer work effectively for RPP installation. Therefore, a crawler mounted rig with pseudo vibratory hammer (model: Casagrande M9-1) was utilized to install the RPPs. However, the rig was not suitable due to the steepness of the slope at the crest. There might be a chance of tilting of the rig and therefore, the work was stopped because of the safety issue.

The installation work was further resumed with an excavator equipped with Hydraulic breaker (model: deer 200D with FRD, F22 hydraulic hammer). The excavator performed well in terms of safety issue and the installation was continued for two days.

The Mockingbird slope had repetitive failures. Previously, the slope was stabilized with lime during TxDOT maintenance operation and at some location of the slope, the soil was very stiff. As a result, the RPP counter very stiff zone at several points where it cannot penetrate. As a result, the RPP buckled and broke down during the

installation which was considered as refusal. Thus, a total of 130 RPPs were installed in the Mockingbird slope. Figure 4-3 shows the RPP instillation at I-35.



Figure 4-3 RPP instillation at I-35

Second phase of RPP instillation followed in October 2014. Caterpillar rig model number CAT 32D LLR was used with the hydraulic hammer CAT H130S was used to install the RPPs at I-35. Pin installation was carried out during month of October which experienced the drought season in the entire Texas region, followed by the driest summer. Hence, during the time of the pin installation, soil conditions were extremely dry and very stiff to hard in consistency. Two masking molds were prepared to mount in the hydraulic hammer with iron chain or straps to connect either the iron pins or the RPPs. One mold was welded with the iron nail as shown in Figure 4-3. Iron nail was hammered into the ground initially so that RPPs could be installed easily. Iron nail had same cross-sectional area as the RPP.

During second phase of instillation a total of 121 RPPs were installed whereas during the first phase total of 130 RPPs were installed. As a result a total of 251 RPPs were installed to stabilize the slope at Mockingbird site. The layout of the as-built reinforcement section is presented in Figure 4-4

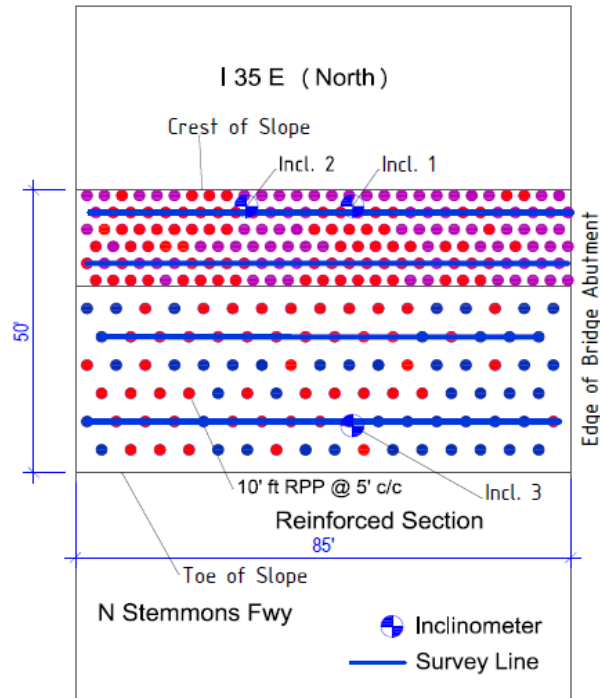


Figure 4-4 As-Built RPP layout of I-35 slope

4.3 Performance Monitoring of I-35 Slope

The inclinometers at the Mockingbird lane slope were monitored on a bi-weekly basis. The topographic survey over the slope was conducted on monthly basis. In addition, the contour survey of the slope was also performed in quarterly basis. The performance monitoring results for the Mockingbird slope are summarized

4.3.1 Inclinometer

The inclinometers were monitored on a bi-weekly basis, and the horizontal movements of the inclinometers are included. Locations of the inclinometers are presented in Figure 4-4. The cumulative displacements with time for Inclinometers I-1 through I-3 are presented in Figures 4-5 through 4-7.

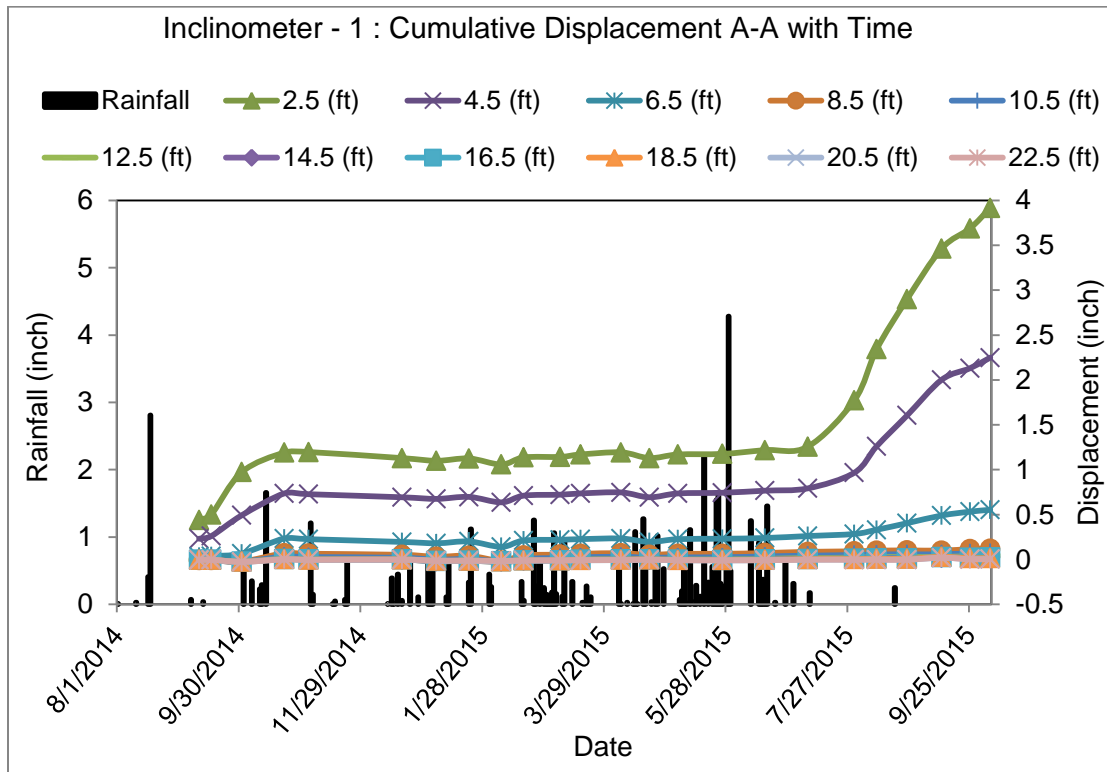


Figure 4-5 Displacement in inclinometer 1 at I-35

In Inclinometer I-1, after the second phase of the instillation during September 2015 at I-35, the movement of the slope is constant at approximately 1.25 inches at upper 2.5 feet. In addition, movement at the deeper depth is also constant, indicating that the movement of the slope has gradually stabilized.

Similarly, movements at Inclinometer I-2 and I-3 are negligible which also indicated that the movement at the slope has stabilized as shown in Figures 4-6 and 4-7.

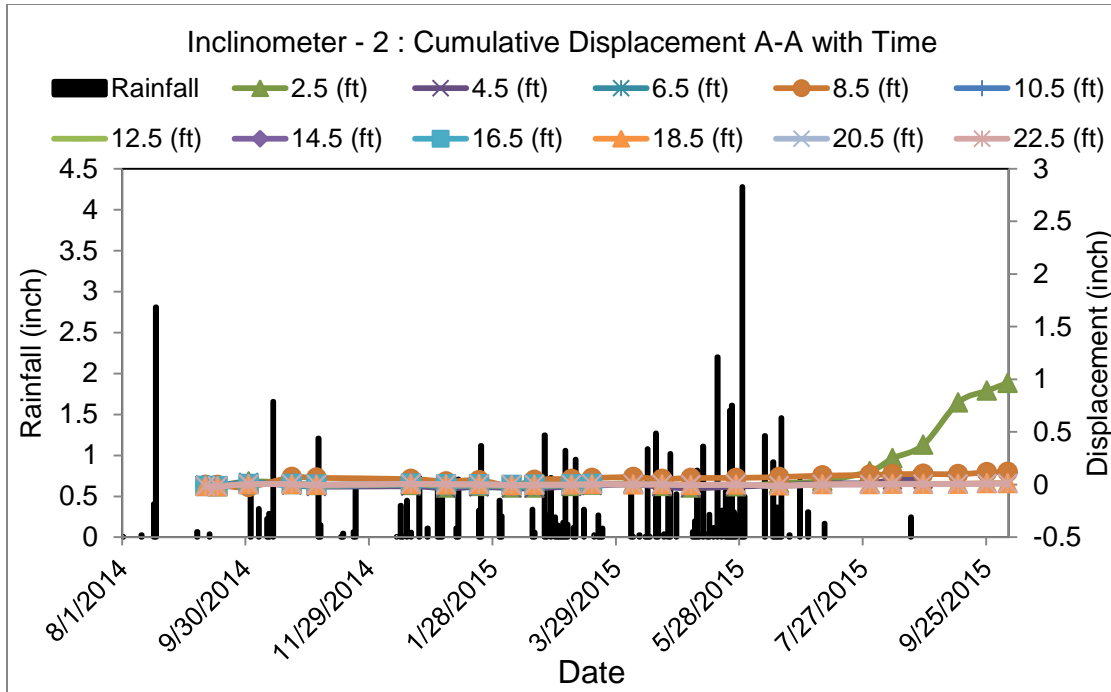


Figure 4-6 Displacement in inclinometer 2 at I-35

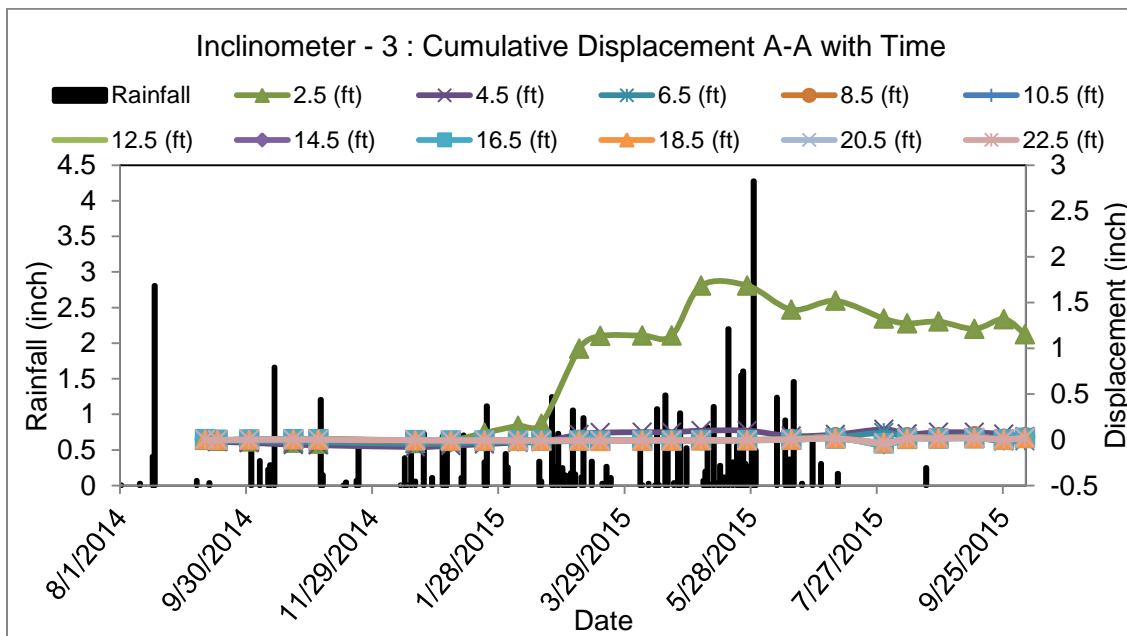


Figure 4-7 Displacement in inclinometer 3 at I-35

4.3.2 Topographic Survey

The total settlement over the crest at Mockingbird Slope was measured monthly during each site visit. The total settlement plot presented that there was no significant settlement at the crest. The maximum settlement was approximately 5 inches toward the location where the cracks appeared during removal of drilled shaft. The total settlement plot presented the lowest settlement was in good agreement with the numerical modeling performed in previous task. The result of the Topographic Survey is presented in Figure 4-8.

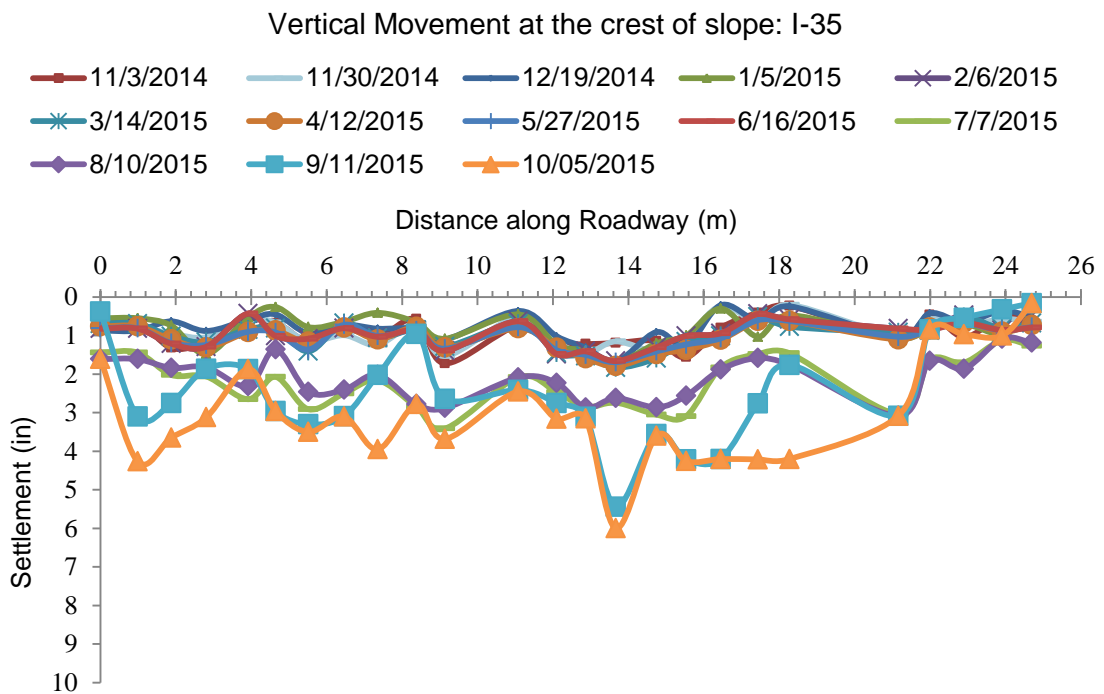
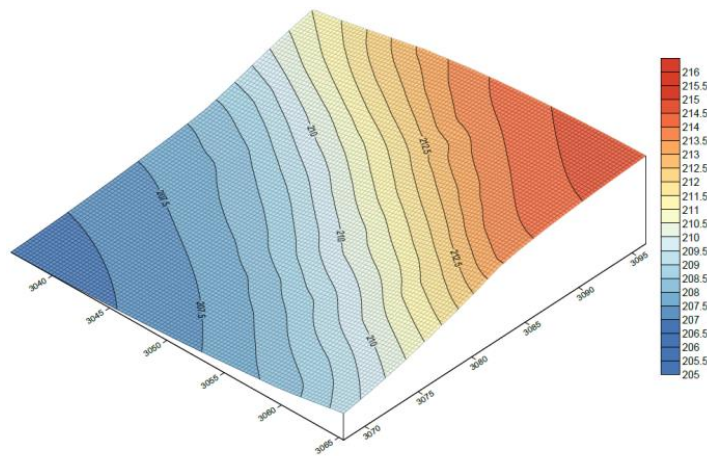


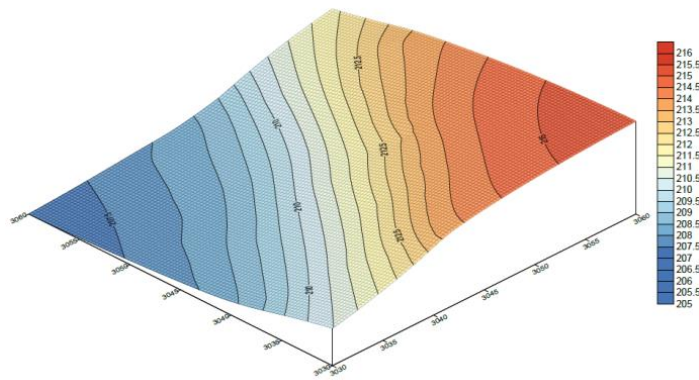
Figure 4-8 Settlement at the crest of the I-35 Slope

4.3.3 Contour Survey

Contour Survey of the Mockingbird slope was also performed to monitor the slope movement. Based on the contour survey, there was no substantial movement of the slope. The contour survey of Mockingbird slopes is presented in Figure 4-9. Contour Survey was plotted using the surfer program. Based on the contour survey, slope movement was not observed during this period.



(a)



(b)

Figure 4-9 Contour Survey at I-35 Slope, (a) Survey on January 5, 2015, (b) Survey Performed on June 14, 2015

4.4 Slope Stabilization at SH 183 Slope

A section (60 feet x 90 feet) of the slope was stabilized using the RPP of 10 feet long at 3 feet center to center at the upper 30 feet of the slope and the remaining of the slope had the RPP spacing of 4 feet center to center. All the RPP installed at the SH 183 were designed as 10 feet long. The design layout and cross-section of the slope are presented in Figures 4-10 and 4-11, respectively.

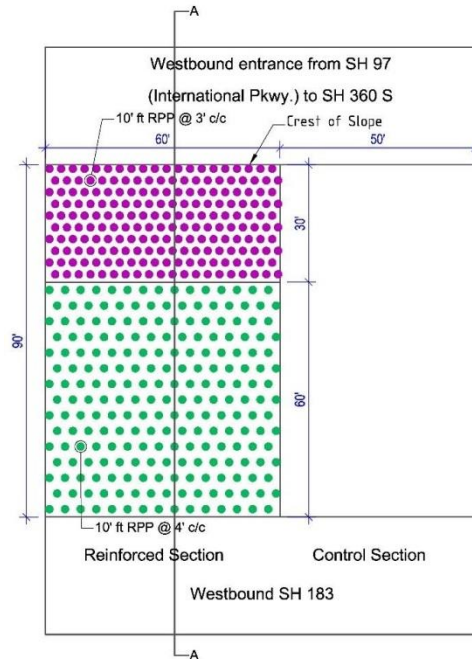


Figure 4-10 Plan View of RPP layout at SH 183 slope

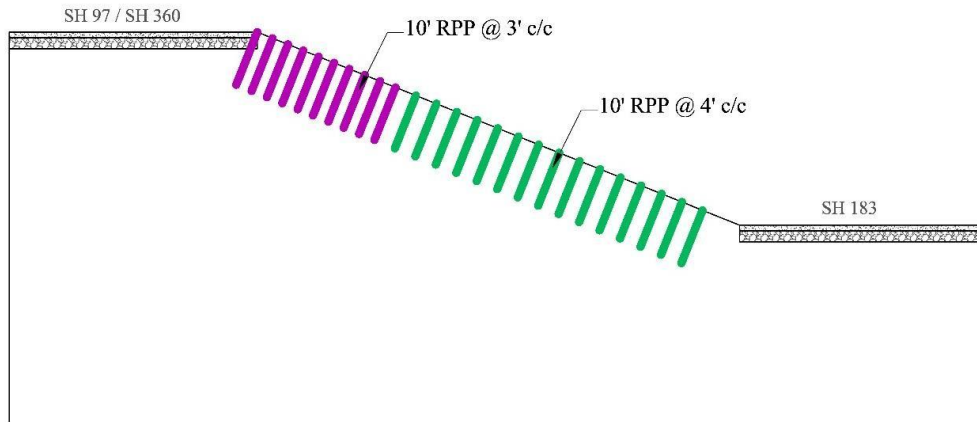


Figure 4-11 Section A-A of RPP layout at SH 183 Slope

4.5 RPP instillation at SH-183 Slope

RPP were installed during September 2014, which was right after the driest summer which experienced the drought season in the entire Texas region. Hence, during the time of the RPP installation, soil conditions were extremely dry and very stiff to hard in consistency. The regular method of driving RPP into the ground resulted in the breakage of RPP in the hard soil. As a result with few trials, a steel pin was introduced. The steel pin was attached with the hammer and used to make hole in the stiff soil layer up to 7 feet, by driving it in the ground. Later, the steel pin was removed and RPP was driving immediately after the steel pin. This procedure of installation worked well and a total of 425 RPPs were installed at SH 183 slope. RPP instillation photo are presented in Figure 4-12



Figure 4-12 RPP Instillation at SH 183 Slope

There was some section at the slope where RPP could not be installed due to the previous retaining system present at the slope. The as build layout of the slope is presented in Figure 4-13 and the numerical modeling of the as built section 1-1 and section 2-2 are presented in Figure 4-14(a) and 4-14(b). The as built factor of safety for section 1-1 and section 2-2 were 1.62 and 1.61, respectively

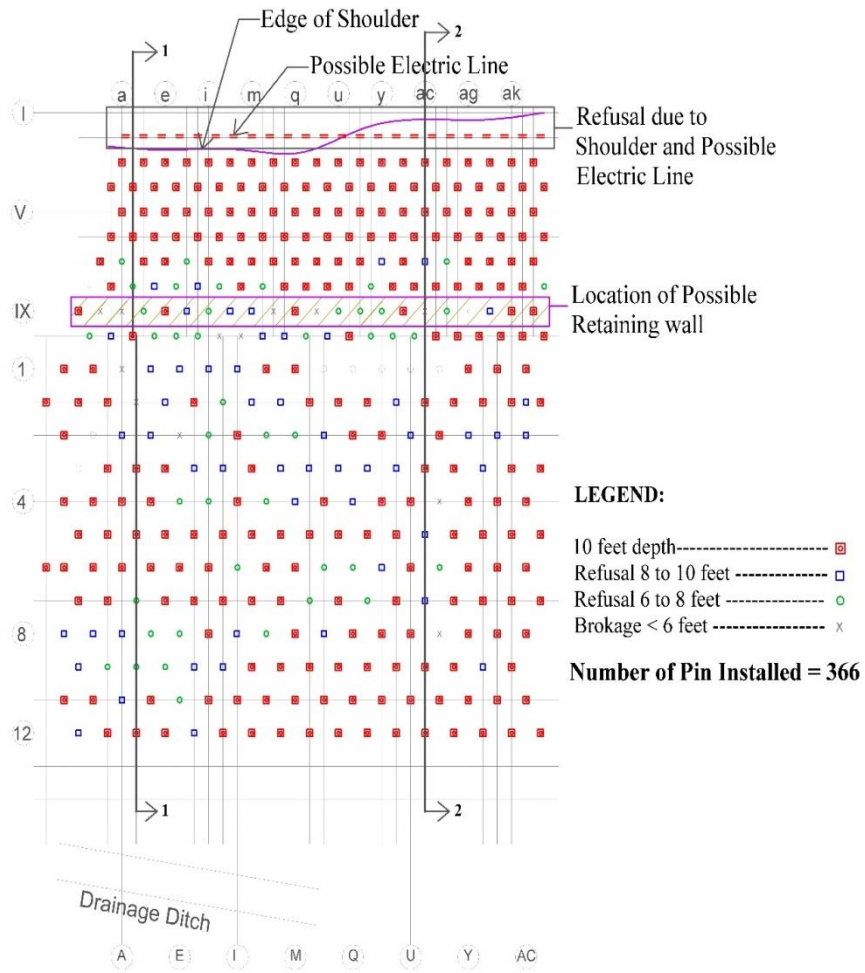
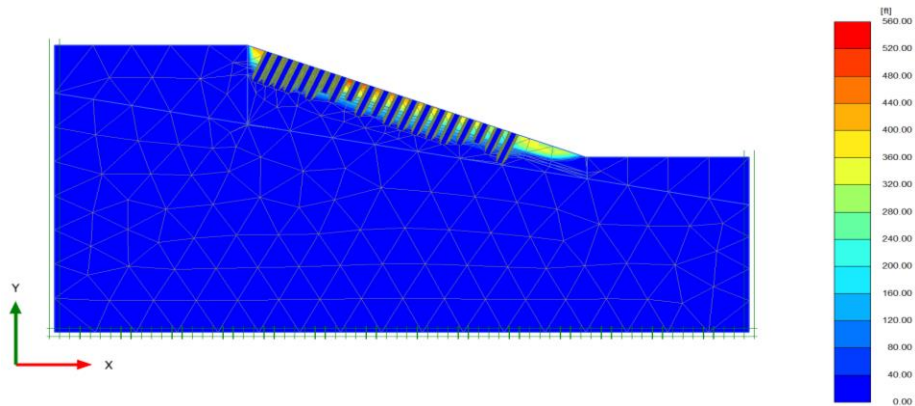
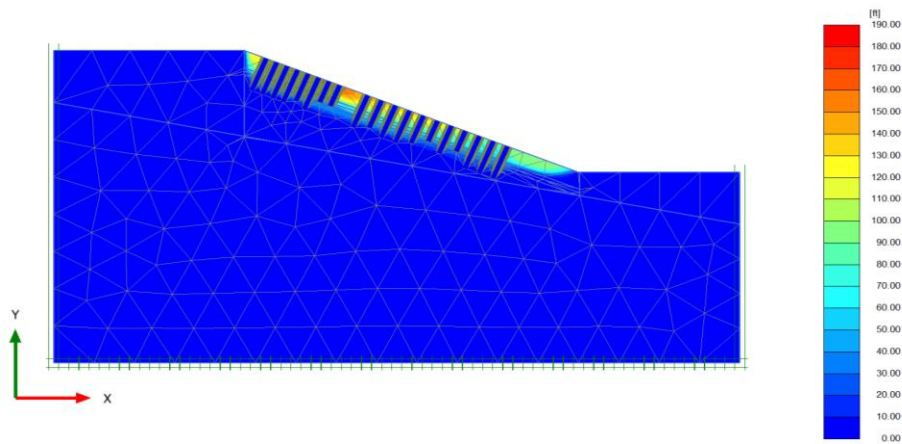


Figure 4-13 As Built Layout of SH 183



(a) Section 1-1, FOS 1.62



(b) Section 2-2, FOS 1.61

Figure 4-14 As built Slope Stability analysis of (a) Section 1-1 and
(b) Section 2-2

4.6 Performance Monitoring of SH 183 Slope

The topographic survey was conducted on monthly basis to observe the movement of the RPP at SH 183 slope. In addition, the contour survey of the slope was also performed in quarterly basis. The rainfall data from the DFW airport were also collected from the weather stations and plotted to observe the correlation of the slope movement. The performance monitoring results for SH 183 slope is summarized.

4.6.1 Topographic Survey

The total settlement over the crest of the slope was measured during each survey and plotted result is presented in Figure 4-15. The maximum settlement was about 1.5 inches toward the abutment of the bridge. The total settlement plot presented that there was not significant settlement at the crest. The total settlement plot presented the lowest settlement was in good agreement with the numerical modeling performed in previous section.

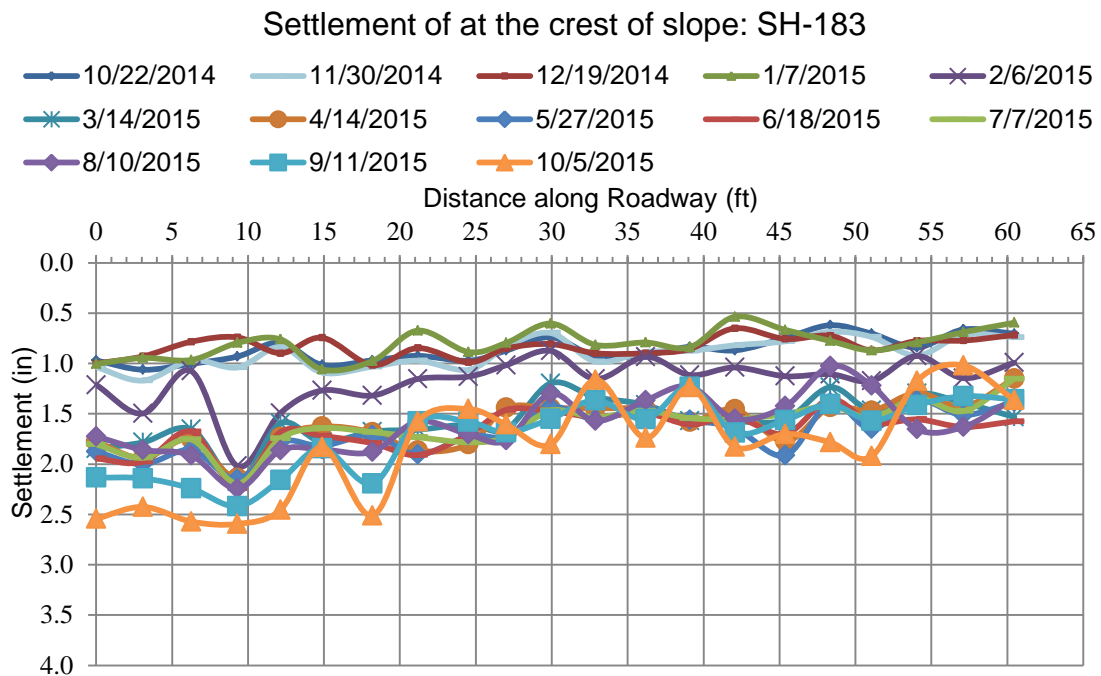
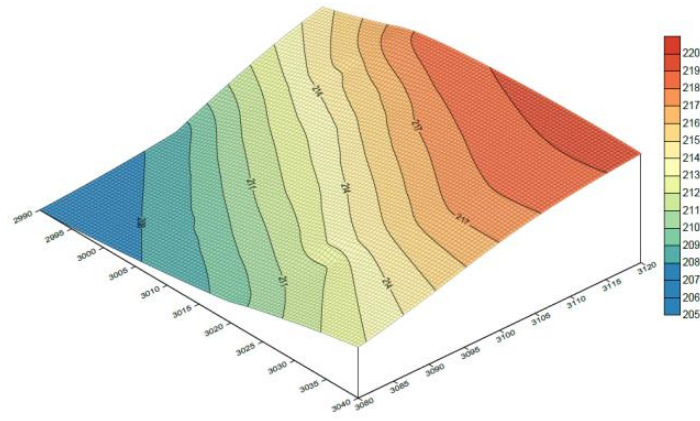


Figure 4-15 Settlement at the crest of the SH-183 Slope

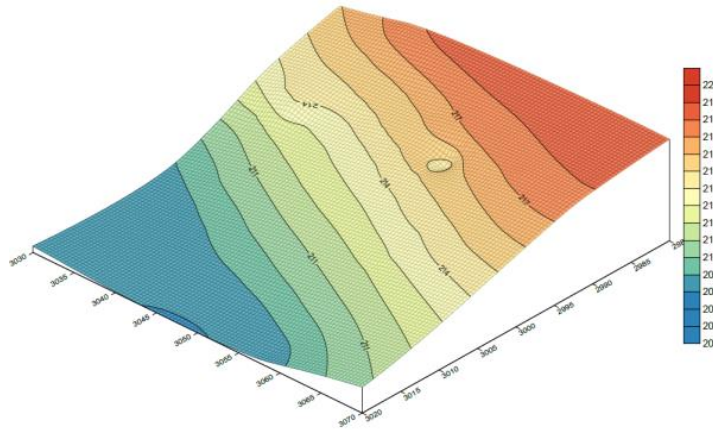
4.6.2 Contour Survey

Contour Survey of the SH 183 slope was also performed quarterly basis to monitor the slope movement. Based on the contour survey, there was no substantial movement of the slope. However, there was little dip observed at the area where pins

could not be installed due to the previous retaining structure. In addition, some movements were observed close to the abutment of the bridge which verifies the results of the topographic survey. The contour survey of the SH 183 slope is presented in Figures 4-16(a) and 4-16(b).



(a)



(b)

Figure 4-16 Contour Survey at SH-183 Slope, (a) Survey on January 7, 2015, (b) Survey Performed on June 14, 2015

4.7 Lesson learned from instillation process

Modification to the conventional rig was made to attach the hydraulic hammer as shown in Figure 4-17. Bucket from the rig was removed and a hydraulic hammer was placed to push the plastic pins into the ground. The track rig is suitable for the installation process over the slopes, as no additional anchorage is required to maintain the stability of the equipment, which reduces labor, cost and time of the installation process. It should be noted that the slope of the embankment were approximately 1:3 hence, hence the pin installation process was especially complex without the track rig.



Figure 4-17 Conventional rig with hydraulic hammer

On the other hand, equipment should be readily available and commonly used in the construction industry. So, that budget is not allocated for the purchase of the special equipment.

Caterpillar rig model number CAT 32D LLR was used with the hydraulic hammer CAT H130S was used to install the RPPs at I-35 and SH 183 projects. In addition, two masking molds were prepared to mount in the hydraulic hammer with iron chain or straps to connect either the iron pins or the RPPs. One mold was welded with the iron pin as shown in Figure 4-18. Iron nail was hammered into the ground initially so that RPPs could be installed easily. Iron nail had same cross-sectional area as the RPP.



Figure 4-18 Iron nail being hammered into ground

Pin installation was carried out during month of September and October which experienced the drought season in the entire Texas region, followed by the driest summer. Hence, during the time of the pin installation, soil conditions were extremely dry and very stiff to hard in consistency. First couple of attempt of push the RPPs into the ground without any iron nail failed. So, attempts were made to hammer the iron nail that

were the same cross-sectional area and later push the RPPs into the same hole. Each hole was hammered to the depth of eight (8) feet using the iron nail and later the RPP was inserted to the depth of ten (10) feet below grade. Driving time was measured for both iron nail and RPP during the installation process. Based on the measured driving time, the average installation time, as well as the driving rate, is summarized in Table

Table 4-1 Average RPP driving time

Location of RPP	Length of RPP (ft.)	RPP Spacing (ft.)	Average iron nail hammering time (mins)	Average RPP Driving Time (mins)	Final Average Pin Installation Time (mins)
W/out using Hammer	10	4	-	22.33	22.33
			2.92	2.71	5.64
Using Hammer	10	3 to 4	1.40	1.60	3.00
			0.93	1.23	2.16
			0.49	1.32	1.81
			1.31	1.36	2.67

Initially few plastic pins were hammered into the ground at the toe of the slope without using the iron nail. However, this method ended soon as pins broke off due the high resistance from the stiff soil. So, the iron nail with cross-section size of the RPP was constructed to hammer into the ground up to the depth of 8 feet and then drive the RPP in the same hole. Using this method, the process of installing the pins was efficient and fewer pins were damaged while driving the pins.

Driving time for the pins without hammering the iron nail was 22.33 minutes per pin. However, final pin installation time using the iron nail was between 1.81 and 5.64 minutes per pin. In the beginning, operators were having tough time to install the pins at the slope hence the longer time to hammer the iron nail and then drive the pins.

Average time to hammer the iron nail into the ground was between 0.49 and 2.92 minutes per hole. In addition, the time to drive the 10 feet RPPs into the ground ranged between 1.23 and 2.71 minutes. These time includes the installation time and to maneuver the rig to the next points. At a time about 20 to 25 points would be hammered which are in the close approximately and the mold would be changed to drive the RPPs in the ground. In a day, approximately 100 pins can be installed if worked without any disturbance like equipment breakage and weather permitted.

Chapter 5

Conclusion and Recommendation for Future Research

5.1 Summary and Conclusion

Reinforced sections at both of the slopes were selected as reference slope and the performance of the reinforced sections were calibrated during numerical study. The field performance of the reinforced sections were evaluated and compared with the numerical model. The numerical study presented that the predicated and observed performance were in good agreement. Based on the previous study performed in US 287, all the RPP were kept at a constant length of 10 feet and upper one-third section of the slope was kept at close spacing of 3 feet c/c. However, the bottom two-third sections of the reinforced section were kept at 4 feet c/c at SH-183 and 5 feet c/c at I-35 slope.

Both of the slopes were modeled in PLAXIS using the soil parameters obtained from site specific geotechnical investigation. Based on the numerical modeling, the numbers of RPP were determined. Sections of slope at each slope were reinforced with RPP and the performance of the slope was monitored using inclinometer and surveying instruments.

Based on the design methods, the calculated factors of safeties were in good agreement with the safety analysis results in numerical modeling.

5.2 Recommendation for Future Research

Following recommendation are presented for future studies in regards to the RPP.

1. Performance of the RPP has not been monitored for long term. So, continuous monitoring of the performance of the slope is recommended.

2. Correlation of Creep properties of the soil in association with the RPP in the field could be obtained when performance of the slope is monitored for long term.
3. Detailed cost benefit of using RPP in comparison of other retaining structures is recommended for future studies.
4. Three dimensional numerical model considering the group of the RPP is recommended for future research.

References

Khan, S. (2013) "Sustainable Slope Stabilization Using Recycled Plastic Pin in Texas". Ph.D. Dissertation, The University of Texas at Arlington, Arlington, Texas.

Abramson, L., Lee, T., Sharma, S., and Boyce, G., (2002). Slope Stability and Stabilization Methods, John Wiley, New York, 712 p.

Berg, R. R., Christopher, B. R., & Samtani, N. C. (2009). Design of Mechanically Stabilized Earth Walls and Reinforced Soil Slopes—Volume II (No. FHWA-NHI-10-025).

Bowders, J. J., Loehr, J. E., Salim, H., & Chen, C. W. (2003). Engineering properties of recycled plastic pins for slope stabilization. *Transportation Research Record: Journal of the Transportation Research Board*, 1849(1), 39-46.

Chen, C. W., Salim, H., Bowders, J., Loehr, E., and Owen, J. (2007). "Creep Behavior of Recycled Plastic Lumber in Slope Stabilization Applications" *J. Mater. Civ. Eng.*, 19(2), 130-138.

Hossain, J. (2012). "Geohazard Potential of Rainfall Induced Slope Failure on Expansive Clay". Ph.D. Dissertation, The University of Texas at Arlington, Arlington, Texas.

Golam K. et al. (2014), "Influence of Soil Reinforcement on Horizontal Displacement of MSE Wall". *International Journal of Geomechanics*, Vol. 14, No. 1, February 1, 2014.

Loehr, J. E., Bowders, J., Owen, J., Sommers, L., & Liew, L. (2000). Stabilization of slopes using recycled plastic pins. *Transportation Research Board : Transportation Research Record*, 1-8.

Loehr, J. E., and Bowders, J. J. (2007). "Slope Stabilization using Recycled Plastic Pins – Phase III", Final Report: RI98-007D, Missouri Department of Transportation, Jefferson City, Missouri.

Sommers, L., Loehr, J. E., & Bowders, J. J. (2000). Construction Methods for Slope Stabilization with Recycled Plastic Pins. Proc. Mid-Continent Transportation Symposium 2000. Iowa State University, Ames, Iowa, May 15-16, 2000.

McCormic, W., and Short, R., (2006). "Cost Effective Stabilization of Cley Slopes and Faulure using Plate Piles", Proco., IAEG2006, The Geological Society of London, London, United Kingdom, 1-7.

Quintanar, F.P., (2014) " Development of a Comprehensive Database and Selection Model for Optimum Retaining Wall Construction Cost and Production" Thesis, The University of Texas at Arlington, Arlington, Texas.

Day, R. W., & Axten, G. W. (1989). Surficial stability of compacted clay slopes. *J. of Geotech. Engg.*, 115(4), 577-580.

Day, R. W. (1996). Design and Repair for Surficial Slope Failures. *Practice Periodical on Structural Design and Construction*, 1(3), 83-87.

Evans, D. A. (1972). Slope Stability Report. Slope Stability Committee, Department of Building and Safety, Los Angeles, CA.

Fay, L., Akin, M., & Shi, X. (2012). Cost-Effective and Sustainable Road Slope Stabilization and Erosion Control (Vol. 430). Transportation Research Board, Washington, D.C.

ASCE Seminar (2013): "Earth Retaining Structures, Selection, Design, Construction and Inspection", Pittsburgh, PA / November 7-8, 2013

Braja M. Das. (2011). "Principles of Foundation Engineering". Seventh Edition. Cengage Learning Engineering. Stamford, CT.

Gopu, V. K. and Seals, R. K., (1999), "Mechanical Properties of Recycled Plastic Lumber and Implications in Structural Design". *Composites Institute's, International Conference Proceedings*. CRC Pressl Llc, 1999. Session 7-c/1 to Session & 7-c/6

Gray, D.H. and Sotir, R. B. (1996). "Biotechnical and Soil Bioengineering Slope Stabilization: A Practical Guide for Erosion Control", John Wiley & Sons, New York, N.Y.

Hossain M. S. et al. (2012). "Effects of Backfill Soil on Excessive Movement of MSE Wall". *Journal of Performance of Constructed Facilities*, Vol. 26, No. 6, December 1, 2012.

Loehr, J. E., Fennessey, T. W., & Bowders, J. J. (2007). Stabilization of surficial slides using recycled plastic reinforcement. *Transportation Research Record: Transportation Research Record*, 1989(1), 79-87.

Lynch, J. K., Nosker, T. J., Renfree, R. W., Krishnaswamy, P., & Francini, R. (2001). Weathering effects on mechanical properties of recycled HDPE based plastic lumber. *Proc. ANTEC 2001*, Dallas, Texas, May 6-10.

Short, R. and Collins, B.D., (2006), "Testing and Evaluation of Driven Plate Piles in Full-Size Test Slope: New Method for Stabilizing Shallow Landslides", TRB 85th Annual Meeting Compendium of Papers CD-ROM, January 22-26, Washington D.C

Titi, H., & Helwany, S. (2007). Investigation of Vertical Members to Resist Surficial Slope Instabilities (No. WHRP 07-03). Wisconsin Department of Transportation, Madison, WI.

Biographical Information

Sandip Tamrakar was born in Kathmandu, Nepal on August 1st, 1986. He is the eldest son of Mr. Gopi Tamrakar and Late Mrs. Ganga Tamrakar. After completing his high school in Kathmandu, Nepal he came to USA for higher studies. He received his B.S. Degrees in Civil Engineering with specialization in Geotechnical from the University of Texas at Arlington in December 2011.

Once graduated, he joined consulting firm in Dallas, Texas and gained experience in design and forensic investigation. He was integral part of geotechnical and geophysical investigation on range of projects. After working over two years as Staff Engineer, the author joined University of Texas at Arlington to pursue graduate studies in Geotechnical Engineering under Dr. Sahadat Hossain and his prestigious research group.

The author's research interests include soil and rock slope stability analysis, shallow and deep foundation, retaining structures, geophysical investigation and forensic investigations.

Additionally to the technical and research, the author's interests include Leadership and Business Development Strategies.